Experimental and Chemical Kinetics Study of the Effects of Halon 1211 (CF 2 BrCl) on the Laminar Flame Speed and Ignition of Light Hydrocarbons

ARTICLE *in* THE JOURNAL OF PHYSICAL CHEMISTRY A · MARCH 2015

Impact Factor: 2.69 · DOI: 10.1021/acs.jpca.5b00959 · Source: PubMed

4 AUTHORS, INCLUDING:

Olivier Mathieu

Texas A&M University

40 PUBLICATIONS **275** CITATIONS

SEE PROFILE

THE JOURNAL OF PHYSICAL CHEMISTRY A

Article

pubs.acs.org/JPCA

Experimental and Chemical Kinetics Study of the Effects of Halon 1211 (CF_2BrCl) on the Laminar Flame Speed and Ignition of Light Hydrocarbons

Olivier Mathieu, Charles Keesee, Claire Gregoire, and Eric L. Petersen*

Department of Mechanical Engineering, Texas A&M University, College Station, Texas 77843 , United States

Supporting Information

ABSTRACT: In this study, the effect of Halon 1211 (CF_2BrCl) on the ignition delay time and laminar flame speed of CH_4, C_2H_4, and C_3H_8 were investigated experimentally for the first time. The results showed that the effects of Halon 1211 on the ignition delay time are strongly dependent on the hydrocarbon: the ignition delay time of CH_4 is significantly decreased by Halon 1211 addition, while a significant increase in the ignition delay time was observed with C_2H_4 for the lowest temperatures investigated. Ignition delay times for C_3H_8 were slightly increased, mostly on the low-temperature side and for the fuel-rich case. A significant reduction in the laminar flame speed was observed for all of the fuels. A tentative chemical kinetics model was assembled from existing models and completed with reactions that have been determined in the literature or estimated when necessary. The experimental results were reproduced satisfactorily by the model, and a chemical analysis showed that most of the effects of Halon 1211 on the ignition delay times of C_2H_4 and C_3H_8 are due to the consumption of H radical through the reaction $HBr + H \rightleftarrows Br + H_2$. In the case of methane, the CF_2 radical promotes the formation of H via $CF_2 + CH_3 \rightleftarrows CH_2{:}CF_2 + H$, which then promotes the branching reaction $H + O_2 \rightleftarrows OH + O$. The laminar flame speed results can be explained using catalytic cycles involving Br atoms that are similar to those reported in the literature for CF_3Br. This study exhibits the need for a better estimation of the chlorine atom chemistry during the combustion of hydrocarbons in the presence of fire suppressants.

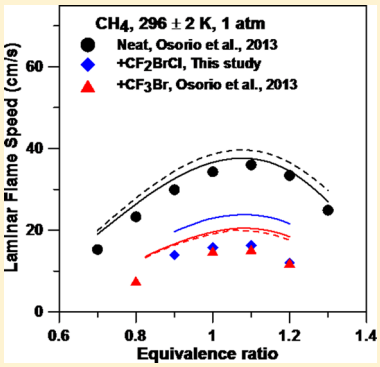

1. INTRODUCTION

Because of their ozone-depleting properties,[1,2] many efficient fire suppressants have been phased out by the Montreal Protocol.[3] Among the agents that have been banned, CF_3Br (Halon 1301) and CF_2BrCl (Halon 1211) were important because of both their efficiency and low toxicity, explaining their large usage. Despite the Montreal Protocol, the concentration of CF_2BrCl in the stratosphere was still increasing more than 10 years after it was banned in developed countries[4,5] as a result of its production in developing countries[6] and use throughout the world. Indeed, even if the production of Halon 1211 has stopped in developed countries, its usage is still allowed through recycling of the existing supply.[7] As a result, Halon 1211 is still currently employed in many applications, notably in the military and aviation areas.

To limit the use of Halon 1211 to the most efficient and strictly necessary applications and to find needed suitable replacements, it is necessary to understand the details of its chemical effects during combustion. Of course, if the detailed chemistry of the suppressant mechanism were known, it would then be possible to try to develop agents or a blend of agents with similar chemical mechanisms but without the ozone-depletion issue. To this end, CF_3Br has been the topic of numerous studies, both numerical[8−12] and experimental.[13−16] However, to the best of the authors' knowledge, there is very little information available in the literature on the combustion chemistry of Halon 1211 alone or with any fuel. The effect of various inhibitors, including CF_2BrCl, on the flame speed of hydrogen was observed by Miller and co-workers.[17] While the method they employed used several assumptions that were not fully valid, the results could be discussed qualitatively and showed that Halon 1211 is an effective fire suppressant. A similar conclusion was reached by Bajpai[18] with diffusion flames and by Zegers et al.[19] with both non-premixed counterflow (with propane/air) and cup burner (with *n*-heptane) flames. The effects of CF_3Br and CF_2BrCl were also studied with *n*-butane combustion, but only at low temperatures (573−673 K).[20] Finally, it is worth mentioning that except for the studies by Yu et al. on the high-temperature pyrolysis of CF_2BrCl with[21] and without[23] hydrogen, no studies are available describing the detailed chemistry of Halon 1211 under practical combustion conditions.

The aim of the work in this paper was twofold. First, the effects of Halon 1211 on important combustion properties (specifically the laminar flame speed (S_L^0) and ignition delay time (τ_{ign})) were investigated for light hydrocarbons of interest

Special Issue: 100 Years of Combustion Kinetics at Argonne: A Festschrift for Lawrence B. Harding, Joe V. Michael, and Albert F. Wagner

Received: January 29, 2015
Revised: March 24, 2015

DOI: 10.1021/acs.jpca.5b00959
J. Phys. Chem. A XXXX, XXX, XXX−XXX

Table 1. Experimental Conditions Investigated behind Reflected Shock Waves for the Present Study

fuel	ϕ	mixture contents (mol %) halon	fuel	O_2	Ar	avg P_5 (atm)	T_5 (K)
			Using Halon 1211 (CF_2BrCl)				
CH_4	0.5	0.04	0.40	1.60	97.96	1.80	1510−1790
	1.0	0.0667	0.667	1.333	97.9333	1.70	1585−2075
	2.0	0.10	1.00	1.00	97.90	1.70	1695−2010
C_2H_4	0.5	0.0286	0.286	1.714	97.9714	2.00	1260−1450
	1.0	0.05	0.50	1.50	97.95	1.96	1300−1575
	2.0	0.08	0.80	1.20	97.92	1.83	1425−1700
C_3H_8	0.5	0.0182	0.182	1.818	97.9818	1.90	1325−1540
	1.0	0.0333	0.333	1.667	97.9667	1.87	1400−1630
	2.0	0.0571	0.571	1.429	97.9429	1.80	1495−1745
			Using Halon 1301 (CF_3Br)				
C_2H_4	0.5	0.0286	0.286	1.714	97.9714	1.95	1255−1555
	1.0	0.05	0.50	1.50	97.95	1.87	1315−1620
	2.0	0.08	0.80	1.20	97.92	1.86	1415−1700

to many industries (namely, CH_4, C_2H_4 and C_3H_8, as in Mathieu et al.[23]). The second objective of the study was then to use these data to develop and validate the first generation of a detailed kinetics model that is able to reproduce the experimental trends and explain the results. The experimental setups are described first, after which the results obtained during the experimental study are presented. The experimental results are then compared with literature data to assess the effects of CF_2BrCl compared with those of other fire suppressants investigated under similar conditions in recent work by the authors. The next part of this paper deals with the description of the proposed model for Halon 1211 oxidation and its validation. Finally, this model is used to explain the effects of Halon 1211 addition on the combustion properties of the hydrocarbons investigated herein.

2. EXPERIMENTAL SETUPS

2.1. Shock Tube. A single-diaphragm stainless steel shock tube was used to determine the ignition delay times behind reflected shock waves of the mixtures highly diluted in Ar. The driven section is 4.72 m long with an i.d. of 15.24 cm, and the driver section is 2.46 m long with an i.d. of 7.62 cm. Details and schematics of the shock-tube setup are provided in Aul et al.[24] The wave speed was measured through five PCB P113A piezoelectric pressure transducers equally spaced alongside the driven section and mounted flush with the inner surface. The incident shock wave velocities were determined using signals delivered by these transducers and four Fluke PM-6666 timer/counter boxes. The incident wave speed at the endwall location was then determined using a curve fit of these four velocities extrapolated to the endwall. Post-reflected-shock conditions were obtained using this extrapolated wave speed in conjunction with one-dimensional shock relations and the initial conditions in the test region. This method was proven to maintain the uncertainty in the temperature determination behind reflected shock waves (T_5) below 10 K.[25] The test pressure was monitored by one PCB 134A transducer located at the endwall and one Kistler 603 B1 transducer located at the sidewall in the same plane as the observation window (sapphire, located 16 mm from the endwall).

Nonideal boundary-layer effects measured by the rate of change in pressure (dP/dt) behind the reflected shock wave were determined to be less than 2% per millisecond for all of the experiments. Because of the dilution level used, these nonideal effects are essentially due to the facility (and not to the heat release). The corresponding increase in temperature for these dP/dt levels would be less than 10 K for the longest ignition delay times reported in this study and therefore does not have a noticeable impact on the results presented herein. Experiments were performed at around 1.8 atm for three equivalence ratios (ϕ): 0.5, 1.0, and 2.0. Polycarbonate diaphragms were used, and a cross-shaped cutter was employed to facilitate breakage of the diaphragm and prevent diaphragm fragments from tearing off. Helium was used as the driver gas during this study.

Prior to every run, the driven section was evacuated to 2×10^{-5} Torr or better using a roughing pump and a Varian 551 turbomolecular pump. The pumping time between experiments was minimized using a pneumatically driven poppet valve matching the inside diameter of the driven section and allowing for a passage with a diameter of 7.62 cm between the vacuum section and the driven tube. The pressure was measured using two MKS Baratron model 626A capacitance manometers (0−10 Torr and 0−1000 Torr) and an ion gauge for high vacuums. Test mixtures were prepared manometrically in a mixing tank with a length of 3.05 m made from stainless steel tubing with an i.d. of 15.24 cm. The pressure in the mixing tanks was measured using a Setra GCT-225 pressure transducer (0−17 atm). The mixing tank was connected to the vacuum system and could be evacuated to pressures below 1×10^{-6} Torr. The gases (CH_4 (99.97%), C_2H_4 (99.995%), O_2 (99.999%), C_3H_8 (99.5%), CF_2BrCl (>99%) and Ar (99.999%)) were passed through a perforated stinger traversing the center of the mixing tank to allow for rapid, turbulent mixing. To further ensure homogeneity through diffusion processes, mixtures were allowed to rest for at least 1 h prior to the first run.

The baseline mixtures, originally investigated by Mathieu et al.,[23] were mixtures of hydrocarbon and oxygen diluted in 98% Ar that were investigated at around 1.8 atm with ϕ = 0.5, 1.0, and 2.0. The mixtures with Halon 1211 investigated in the present study followed the same pattern used in previous studies by the authors' group,[16,23] i.e., using the same baseline mixtures but with CF_2BrCl addition corresponding to 10% of the hydrocarbon's molar concentration (with the CF_2BrCl addition being taken out of the 98% Ar dilution). The mixtures and conditions investigated during this study are provided in Table 1. It should be noted that mixtures of C_2H_4 with CF_3Br were also studied to allow a direct comparison of the results for

DOI: 10.1021/acs.jpca.5b00959
J. Phys. Chem. A XXXX, XXX, XXX−XXX

the additions of CF_3I,[23] CF_3Br, and CF_2BrCl to all of the fuels considered.

The ignition delay time was measured using the chemiluminescence emission from the $A^2\Sigma^+ \rightarrow X^2\Pi$ transition of the excited-state hydroxyl radical (OH*) using an interference filter centered at 307 ± 10 nm with a Hamamatsu 1P21 photomultiplier tube in a custom housing. The ignition delay time is defined herein as the time between the passage of the reflected shock wave, as indicated by a pressure jump in the signal delivered by the sidewall pressure transducer, and the onset of OH* emission, as given by the intersection of the line drawn along the steepest rate of change of OH* de-excitation and the horizontal line defining the zero-concentration level (Figure 1). Time zero is defined as the time of arrival of the reflected shock wave at the sidewall measurement location. All of the data signals were recorded using a 14-bit GageScope digital oscilloscope from Gage Applied Sciences with sampling rates of 1 MHz or greater per channel.

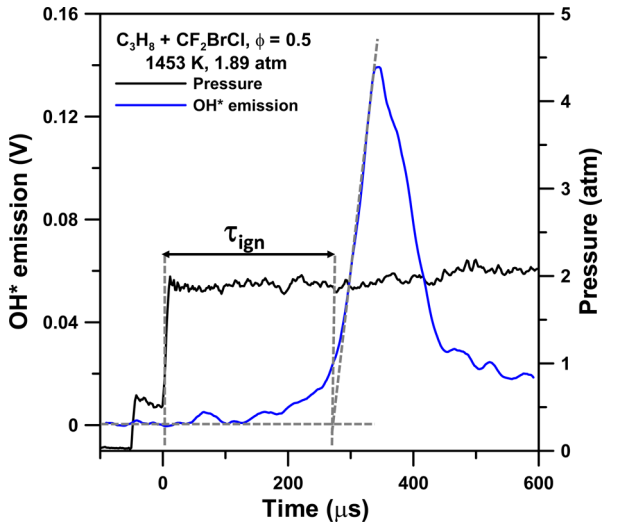

Figure 1. Method for determination of the measured ignition delay time (τ_{ign}). Time zero is defined as the arrival of the reflected shock wave at axis of the observation window, and τ_{ign} is determined using the OH* signal and corresponds to the intersection of lines drawn along the steepest rate-of-change and the zero-concentration level.

Uncertainties in the ignition delay time arise from two sources: the uncertainty in the determination of the temperature behind the reflected shock wave and the uncertainty associated with the determination of the steepest rate of change from the OH* emission profile. The temperature determination is the most important uncertainty, and as mentioned earlier, the experimental setup and method allow a determination of T_5 to within less than 10 K. The second source of uncertainty is typically smaller than the uncertainty in the temperature. Overall, the total uncertainty in τ_{ign} reported in this study is estimated to be around 10% (which also includes the temperature variation corresponding to dP/dt). The measured ignition delay times along with corresponding conditions behind the reflected shock waves are provided in Table S1 in the Supporting Information.

2.2. Laminar Flame Speed Experiment. The cylindrical vessel described by Krejci et al.[26] was used to measure flame speeds of spherically expanding laminar flames. The vessel was made out stainless steel and had an inner diameter of 32 cm and an internal length of 28 cm. A *z*-type schlieren setup was used in conjunction with a high-speed camera (Photron Fastcam SA1.1) to record the flame propagation event. The flame images were processed using an in-house, fully automated, MATLAB-based edge-detection code. Mixtures were prepared using the partial pressures method; all of the gases used were ultrahigh-purity grade. The mixtures were allowed to homogenize inside the vessel for 15 min prior to ignition. Flames up to 12.7 cm in diameter could be measured under near-constant-pressure conditions (<2% increase during the usable part of the experiment), as confirmed by the pressure trace from a high-frequency dynamic pressure transducer installed inside the vessel (e.g., see de Vries et al.[27]). Nevertheless, despite the constant-pressure conditions, the flame speeds of outwardly propagating flames were still affected by ignition and wall confinement (induced by finite chamber size) effects, as reported in Burke et al.[28] To account for these nonidealities, the flame speed values reported herein were extracted only for normalized flame sizes (r_f/r_w, where r_f is the flame radius and r_w is the vessel radius) ranging from 0.12 to 0.30.[28] Because of the relatively large diameter of the vessel, this size range corresponded to flame diameters of 3.8−9.5 cm. Such a size restriction assured that the measured propagation speeds agreed closely with those of an unconfined flame and did not require any additional flow correction since compression-induced burnt gas motion behind the flame was absent.

Spherically expanding flames require extrapolation to zero stretch rate for the unburnt laminar flame speed of a planar flame front, e.g., by using the linear Markstein relationship (eq 1)

$$S_b = S_b^0 - L_{m,b}\kappa \tag{1}$$

in which S_b is the stretched burned-gas flame speed, S_b^0 is the unstretched, burned laminar flame speed, $L_{m,b}$ is the burned-gas Markstein length, and κ is the stretch rate, given by eq 2:

$$\kappa = \frac{2}{r_f}\frac{dr}{dt} \tag{2}$$

where r_f is the flame radius. More sophisticated nonlinear Markstein relationships, NM-I (eq 3) and NM-II (eq 4), have been proposed over the conventional linear Markstein relationship to account for variations in Lewis number (Le):[29]

$$S_b = S_b^0 L_{m,b}\left(\frac{2}{r_f}\right) \tag{3}$$

$$\ln(S_b) = \ln(S_b^0) - S_b^0 L_{m,b}\left(\frac{2}{r_f S_b}\right) \tag{4}$$

It was shown by Chen[29] that failure to use the appropriate nonlinear model could result in significant overprediction of flame speeds and Markstein lengths, for example, by 35% and 283%, respectively, for methane/air at ϕ = 1.34 using the linear correlation. The choice of the appropriate nonlinear model for outwardly propagating flames depends on the Lewis number of the test mixture. NM-I was used for near-unity and positive Lewis numbers ($Le \gg 1$), and NM-II was used for $Le < 1$. The unburned, unstretched flame speed was obtained by multiplying S_b^0 by the density ratio of burned to unburned gas (from equilibrium).

During this study, laminar flame speeds were measured over a large range of equivalence ratios at an initial pressure of 1 atm

DOI: 10.1021/acs.jpca.5b00959
J. Phys. Chem. A XXXX, XXX, XXX−XXX

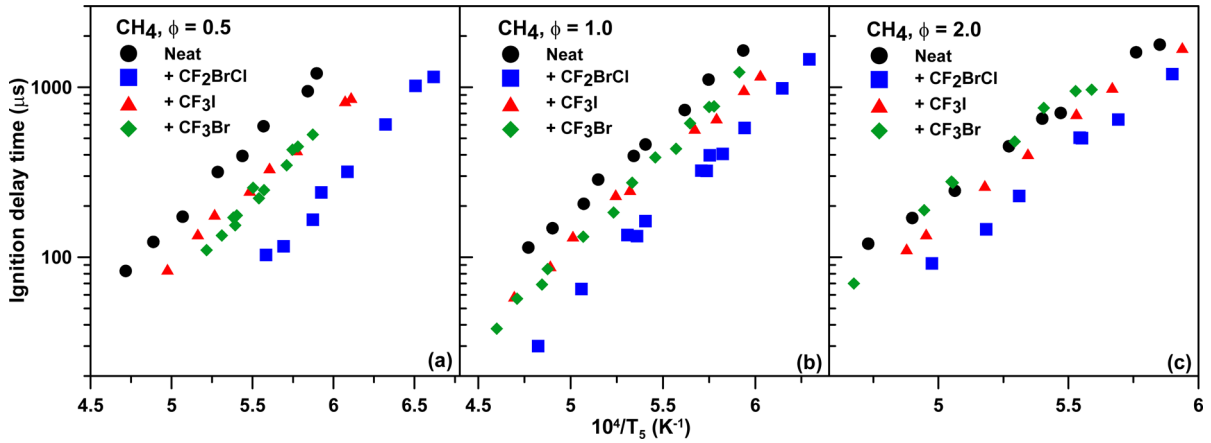

Figure 2. Effect of fire suppressant addition on the ignition delay time of CH_4 at around 1.8 atm for (a) ϕ = 0.5, (b) ϕ =1.0, and (c) ϕ = 2.0. Data for neat CH_4 and CF_3I addition are from Mathieu et al.;[23] data for CF_3Br addition are from Osorio et al.[16]

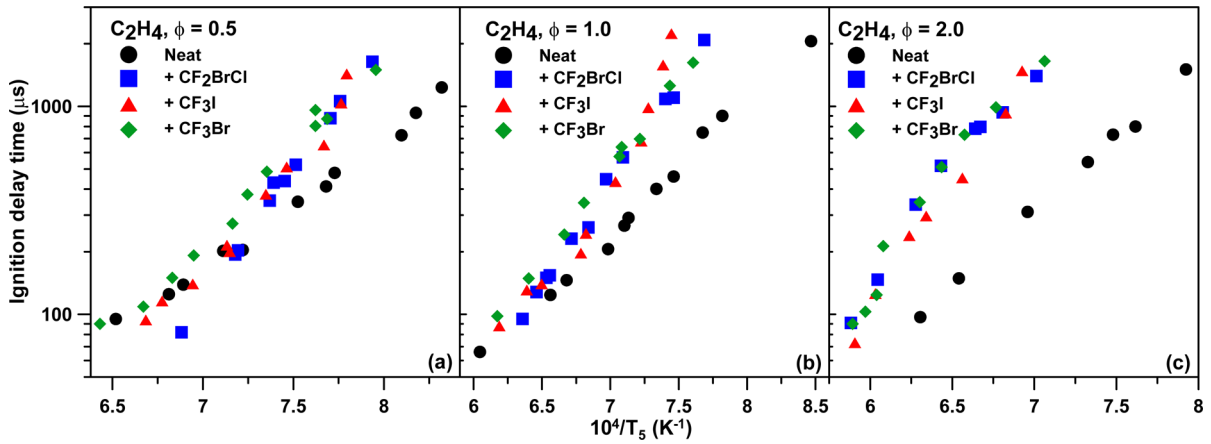

Figure 3. Effect of fire suppressant addition on the ignition delay time of C_2H_4 at around 1.8 atm for (a) ϕ = 0.5, (b) ϕ =1.0, and (c) ϕ = 2.0. Data for neat C_2H_4 and CF_3I addition are from Mathieu et al.[23]

and an initial temperature of 296 ± 2 K. The measured experimental laminar flame speeds are provided in Table S2 in the Supporting Information.

Bias or systematic error (B_{S_L}) and random uncertainty (P_{S_L}) form the total uncertainty, which is computed as $U_{S_L} = (B_{S_L}{}^2 + P_{S_L}{}^2)^{1/2}$. The systematic error is defined as $B_{S_L} = [\sum_i (\partial S_{L,u}(x_i)/\partial x_i) u_i]^{1/2}$, where x_i is an independent variable (i.e., p, T) that affects the flame speed and u_i is the precision with which it can be measured. Since the mixtures were prepared using the partial pressure method, the uncertainty in the pressure is manifested as uncertainty in the equivalence ratio. Herein, u_ϕ and u_T are the manufacturer-specified precisions for the pressure gauge and the thermocouple, respectively. A functional relationship for the flame speed of the form

$$S_{L,u}(x_i) = S_{L,u}(\phi, T) = \left(\sum_{j=0}^{4} a_j \phi^j \right) \left(\frac{T}{298\ \mathrm{K}} \right)^{\left(\sum_{j=0}^{3} b_j \phi^j \right)}$$

was derived for each fuel using COSILAB calculations and was then used to estimate the derivatives of $S_{L,u}$ with respect to ϕ and T. The bias error was then estimated for the different ϕ for all mixtures tested herein. The random or precision uncertainty was calculated from several repetitions of a fixed condition and is defined as $P_{S_L} = (t_{M-1,95\%} S_{S_L})/M^{1/2}$, where M is the sample size, S_{S_L} is the sample standard deviation, and $t_{M-1,95\%}$ is the two-tailed inverse of the Student's t distribution with $M - 1$ degrees of freedom and a 95% confidence interval. The precision uncertainty was calculated using 29 repetitions of methane/air mixtures at ϕ = 1 from an earlier study and was estimated to be 0.27 cm/s. This rigorous approach resulted in an estimated uncertainty of ±1.05 cm/s for the mixtures tested herein.

3. EXPERIMENTAL RESULTS

3.1. Shock-Tube Results. The effect of Halon 1211 on the ignition delay time of the hydrocarbons considered is presented in this section. The effect of CF_2BrCl addition is compared with results from former studies conducted under similar conditions with the addition of CF_3Br[16] and CF_3I.[23]

Effect of Halon 1211 Addition on Methane Ignition. The effect of Halon 1211 on the ignition delay time for methane is shown in Figure 2 at (a) ϕ = 0.5, (b) ϕ = 1.0, and (c) ϕ = 2.0. As can be seen, adding CF_2BrCl to the mixture induces a strong increase in the reactivity: the ignition delay time is decreased by a factor larger than 6 under fuel-lean conditions and by factors of around 3 and 2 for the stoichiometric and fuel-rich cases, respectively. These results were also compared with recent data for CF_3Br and CF_3I addition under similar conditions.[16,23] As can be seen, under the conditions investigated, Halon 1211 has

DOI: 10.1021/acs.jpca.5b00959
J. Phys. Chem. A XXXX, XXX, XXX−XXX

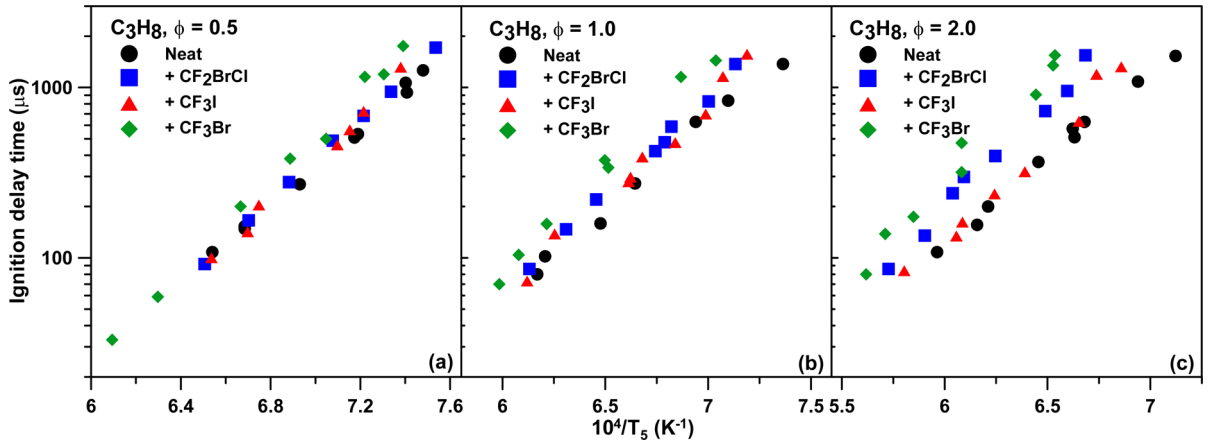

Figure 4. Effect of fire suppressant addition on the ignition delay time of C_3H_8 at around 1.8 atm for (a) ϕ = 0.5, (b) ϕ = 1.0, and (c) ϕ = 2.0. Data for neat CH_4 and CF_3I addition are from Mathieu et al.;[23] data for CF_3Br addition are from Osorio et al.[16]

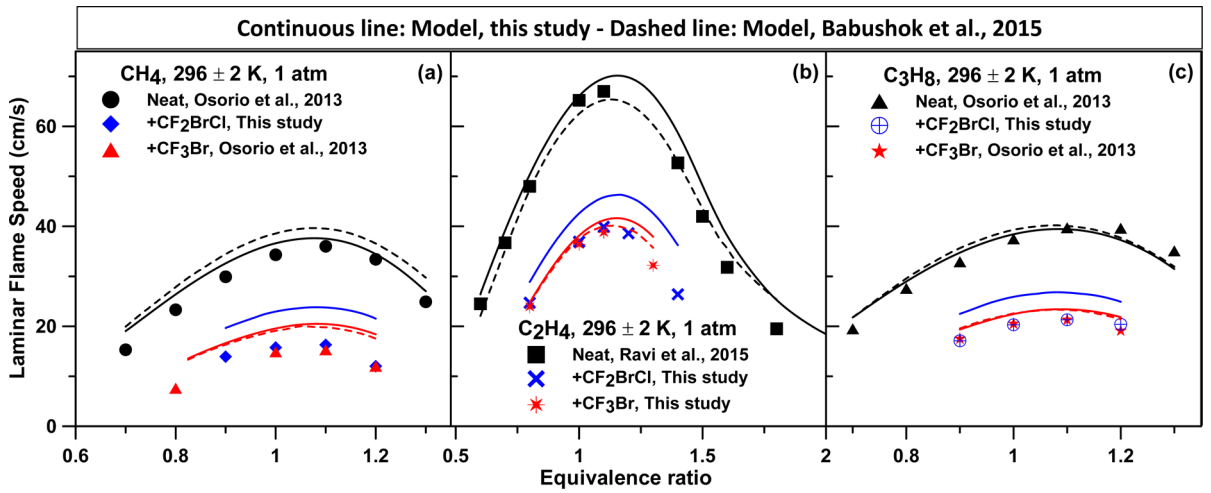

Figure 5. Effect of 1% fire suppressant addition on the laminar flame speeds of (a) CH_4, (b), C_2H_4, and (c) C_3H_8 at an initial pressure of 1 atm and an initial temperature of 296 ± 2 K. Data for neat CH_4 and C_3H_8 mixtures and for CF_3Br addition with CH_4 and C_3H_8 mixtures are from Osorio et al.;[16] data for neat C_2H_4 are from Ravi et al.[30]

a larger effect on methane ignition than both Halon 1301 (CF_3Br) and Halon 13001 (CF_3I), since the ignition delay times for the two other fire suppressants are between those of neat methane and those for methane seeded with CF_2BrCl.

Effect of Halon 1211 Addition on Ethylene Ignition. The effects of CF_2BrCl addition on the ignition of ethylene are shown in Figure 3 for equivalence ratios ranging from 0.5 to 2.0. As can be seen, the addition of Halon 1211 tends to increase the ignition delay time, mostly on the low-temperature side, and this effect grows with increasing equivalence ratio: at the lowest temperature investigated for each set of conditions, the ignition delay time is increased by factors of around 2.4, 2.7, and 4 at ϕ = 0.5, 1.0, and 2.0, respectively. However, it is interesting to note that although the CF_2BrCl addition increases the ignition delay time over the entire range of temperature investigated for the fuel-rich conditions (c), the ignition delay times for the neat and fire-suppressant-addition mixtures are similar at around 1135 K for the stoichiometric case (b), and the ignition delay times are even shortened by the presence of CF_2BrCl above 1380 K at ϕ = 0.5 (a). The results with CF_3I and CF_3Br are very similar to those for Halon 1211; however, one can notice that the increase in the ignition delay time seems greater with CF_3I at low temperature and that the ignition delay time does not seem to be reduced much by CF_3I and CF_3Br on the high-temperature side of the fuel-lean case.

Effect of Halon 1211 Addition on Propane Ignition. Figure 4 presents the effect of CF_2BrCl on C_3H_8 ignition at (a) ϕ = 0.5, (b) ϕ = 1.0, and (c) ϕ = 2.0. As can be seen in this figure, Halon 1211 addition has little influence on the ignition delay time of propane: the results are nearly unchanged at ϕ = 0.5 (a 20% increase is observed on the low-temperature side only), and a small increase in the ignition delay time is observed at ϕ = 1.0 (between 20% at high temperature and 45% at low temperature). For the fuel-rich case, a noticeable increase in the ignition delay time is observed over the entire range of temperature investigated (between a factor of 1.6 at high temperature and a factor of 2.0 at low temperature). By comparison, CF_3Br has a larger effect in increasing the ignition delay time over the range of conditions investigated. The CF_3I-enhanced ignition delay time results are similar to those of CF_2BrCl, except for the fuel-rich case where CF_3I slightly reduces the reactivity of the mixture at the end of the low-temperature side only.

3.2. Laminar Flame Speed Results. As can be seen in Figure 5 for (a) methane, (b) ethylene, and (c) propane, the addition of 1% Halon 1211 to the mixture significantly reduces

DOI: 10.1021/acs.jpca.5b00959
J. Phys. Chem. A XXXX, XXX, XXX−XXX

Table 2. Reactions Added for the Halon 1211 Mechanism; The Rate Coefficient of Each Reaction Is of the Form $k = AT^n \exp(-E_a/RT)$, Where A Is in s^{-1}, $cm^3\ mol^{-1}\ s^{-1}$, or $cm^6\ mol^{-2}\ s^{-1}$ As Appropriate, E_a Is in cal mol^{-1}, As Used by the Modeling Software, and R is the Ideal Gas Constant

reaction	A	n	E_a	ref
$O + CF_2BrCl \rightleftarrows ClO + CF_2Br$	3.5×10^{12}	0	13500	est.[a]
$OH + CF_2BrCl \rightleftarrows CF_2Br + HOCl$	3.5×10^{12}	0	17000	est.[a]
$CF_3 + CF_2BrCl \rightleftarrows CF_2Br + CF_3Cl$	5.0×10^{12}	0	11500	est.[a]
$O + CF_2BrCl \rightleftarrows BrO + CF_2Cl$	3.15×10^{12}	0	11000	est.[a]
$OH + CF_2BrCl \rightleftarrows CF_2Cl + BrOH$	3.15×10^{12}	0	13000	est.[a]
$CF_3 + CF_2BrCl \rightleftarrows CF_2Cl + CF_3Br$	4.5×10^{12}	0	4000	est.[a]
$C_2F_4 + O \rightleftarrows CF_2{:}O + CF_2$	3.93×10^{11}	1.48	0	38[b]
$C_2F_4 + O \rightleftarrows CF_3 + CF{:}O$	6.9×10^{10}	1.48	0	38[b]
$C_2F_4 + H \rightleftarrows CHF_2 + CF_2$	1.73×10^{12}	0	−642	39[c]
$C_2F_4 + H \rightleftarrows CF_3 + CHF$	3.1×10^{11}	0	−642	39[c]
$C_2F_4 + F \rightleftarrows CF_2 + CF_3$	2.89×10^{13}	0	0	40
$CCl_4 + CH_3 \rightleftarrows CH_3Cl + CCl_3$	1.26×10^{12}	0	9900	41
$CCl_4 + C_2H_3 \rightleftarrows C_2H_3Cl + CCl_3$	7.5×10^{12}	0	5500	est.[d]
$CCl_4 + C_2H_5 \rightleftarrows C_2H_5Cl + CCl_3$	2.51×10^{12}	0	10200	42
$CCl_4 + i\text{-}C_3H_7 \rightleftarrows i\text{-}C_3H_7Cl + CCl_3$	1.0×10^{12}	0	10200	41
$i\text{-}C_3H_7Cl \rightleftarrows C_3H_6 + HCl$	7.81×10^{19}	−2.0	60660	est.[e]
$i\text{-}C_3H_7Cl \rightleftarrows i\text{-}C_3H_7 + Cl$	2.35×10^{43}	−8.5	96980	est.[e]
$i\text{-}C_3H_7Cl + H \rightleftarrows i\text{-}C_3H_7 + HCl$	3.0×10^{14}	0	7900	est.[e]
$i\text{-}C_3H_7Cl + OH \rightleftarrows H_2O + C_3H_6Cl$	1.53×10^{7}	2.0	994	est.[e]
$C_2Cl_5 + Cl \rightleftarrows C_2Cl_4 + Cl_2$	2.45×10^{13}	0	0	43
$C_2Cl_5 + Br \rightleftarrows C_2Cl_4 + BrCl$	2.45×10^{13}	0	0	est.[f]
$C_2Cl_6 + Cl \rightleftarrows C_2Cl_5 + Cl_2$	1.32×10^{14}	0	17300	43
$C_2Cl_6 + CCl_3 \rightleftarrows CCl_4 + C_2Cl_5$	8.13×10^{11}	0	14100	43
$C_2Cl_6 \rightleftarrows C_2Cl_5 + Cl$	1.0×10^{16}	0	69200	44
$C_2Cl_6 \rightleftarrows CCl_3 + CCl_3$	6.31×10^{17}	0	68400	45
$C_2Cl_6 \rightleftarrows C_2Cl_4 + Cl_2$	5.01×10^{13}	0	54100	44
$C_2Cl_6 + CH_3 \rightleftarrows CH_3Cl + C_2Cl_5$	6.31×10^{11}	0	10100	46
$HBr + Cl_2 \rightleftarrows HCl + BrCl$	3.0×10^{5}	0	0	47
$HCl + Br_2 \rightleftarrows HBr + BrCl$	3.0×10^{5}	0	0	est.[g]
$BrCl + O \rightleftarrows BrO + Cl$	1.26×10^{13}	0	0	43
$BrCl + O \rightleftarrows Br + ClO$	1.26×10^{13}	0	0	est.[h]
$BrCl + CH_3 \rightleftarrows CH_3Cl + Br$	0.91	0	2087	49
$BrCl + CH_3 \rightleftarrows CH_3Br + Cl$	0.91	0	2087	49
$BrCl + OH \rightleftarrows Br + HOCl$	9.04×10^{11}	0	0	50
$BrCl + OH \rightleftarrows BrOH + Cl$	9.04×10^{11}	0	0	50
$BrCl + H \rightleftarrows Br + HCl$	8.59×10^{13}	0	1170	est.[i]
$BrCl + H \rightleftarrows HBr + Cl$	8.59×10^{13}	0	1170	est.[i]
$CF_2Br + F \rightleftarrows CF_3 + Br$	7.2×10^{13}	0	0	est.[j]
$CF_2Br + O \rightleftarrows CF_2 + BrO$	1.8×10^{13}	0	0	est.[j]
$CF_2Br + H \rightleftarrows CF_2 + HBr$	2.0×10^{13}	0	605	est.[k]
$CF_2Br + CH_3 \rightleftarrows CH_3Br + CF_2$	3.0×10^{12}	0	3030	est.[k]
$CHF_2Br + CH_3 \rightleftarrows CF_2Br + CH_4$	1.0×10^{12}	0	6060	est.[l]
$CHF_2Br + H \rightleftarrows CF_2Br + H_2$	6.62×10^{6}	2.05	5440	est.[l]
$CHF_2Br + OH \rightleftarrows CF_2Br + H_2O$	4.89×10^{6}	1.8	1420	est.[l]
$CF_2Br + CF_2Br \rightleftarrows CF_2Br_2 + CF_2$	2.06×10^{16}	0	5720	est.[m]
$OH + CF_2Br_2 \rightleftarrows CF_2Br + BrOH$	3.16×10^{12}	0	14000	est.[n]
$CH_3 + CF_2Br_2 \rightleftarrows CF_2Br + CH_3Br$	1.05×10^{12}	0	10000	est.[n]
$CF_3 + CF_2Br_2 \rightleftarrows CF_2Br + CF_3Br$	4.5×10^{12}	0	10500	est.[n]
$C_2F_4Cl_2 + H \rightleftarrows C_2F_4Cl + HCl$	1.0×10^{15}	0	30000	est.[o]
$C_2F_4BrCl + H \rightleftarrows C_2F_4Cl + HBr$	1.0×10^{15}	0	30000	est.[o]
$C_2F_4BrCl + CF_3 \rightleftarrows CF_3Br + C_2F_4Cl$	3.0×10^{12}	0	11300	est.[o]
$C_2F_4Br_2 + H \rightleftarrows C_2F_4Br + HBr$	1.0×10^{15}	0	30000	est.[o]
$C_2F_4Br_2 + CF_3 \rightleftarrows CF_3Br + C_2F_4Br$	3.0×10^{12}	0	11300	est.[o]
$C_2F_4Cl_2 + CF_3 \rightleftarrows CF_3Cl + C_2F_4Cl$	3.0×10^{12}	0	11300	est.[o]
$C_2F_4Br + H \rightleftarrows C_2F_4 + HBr$	1.41×10^{21}	−2.4	3630	est.[p]
$C_2F_4Br + H \rightleftarrows C_2HF_4Br$	1.12×10^{47}	−10.8	4100	est.[p]
$C_2F_4Br + O_2 \rightleftarrows CF_2Br + CF_2{:}O + O$	1.3×10^{13}	0	23000	est.[p]
$C_2F_4Br + H \rightleftarrows CHF_2 + CF_2Br$	4.37×10^{16}	−0.746	4360	est.[p]
$C_2F_4Br + H_2O_2 \rightleftarrows C_2HF_4Br + HO_2$	9.0×10^{9}	0	1000	est.[p]

DOI: 10.1021/acs.jpca.5b00959
J. Phys. Chem. A XXXX, XXX, XXX−XXX

Table 2. continued

reaction	A	n	E_a	ref
$C_2F_4Br + O \rightleftarrows CF_2Br + CF{:}O + F$	2.2×10^{13}	0	0	est.[p]
$C_3H_8 + C_2F_4Br \rightleftarrows n\text{-}C_3H_7 + C_2HF_4Br$	3.9×10^{11}	0	7800	est.[p]
$C_3H_8 + C_2F_4Br \rightleftarrows i\text{-}C_3H_7 + C_2HF_4Br$	3.3×10^{11}	0	6100	est.[p]
$C_2F_4Br \rightleftarrows CF_2 + CF_2Br$	4.27×10^{15}	0	56240	est.[p]
$C_2F_4Br + F \rightleftarrows CF_2Br + CF_3$	3.16×10^{13}	0	0	est.[p]
$C_2F_4Br + O \rightleftarrows CF_2{:}O + CF_2Br$	1.1×10^{13}	0	0	est.[p]
$C_2F_4Br + OH \rightleftarrows CF_2Br + CF{:}O + HF$	2.2×10^{13}	0	0	est.[p]
$C_2F_4Br + HO_2 \rightleftarrows CF_2Br + CF_2{:}O + OH$	3.0×10^{13}	0	0	est.[p]
$C_2F_4Br + HO_2 \rightleftarrows C_2HF_4Br + O_2$	3.0×10^{11}	0	0	est.[p]
$C_2F_4Br + CH_2O \rightleftarrows C_2HF_4Br + HCO$	5.5×10^{3}	2.8	5900	est.[p]
$C_2F_4Cl + H \rightleftarrows C_2F_4 + HCl$	1.41×10^{21}	−2.4	3630	est.[p]
$C_2F_4Cl + H \rightleftarrows C_2HF_4Cl$	1.12×10^{47}	−10.8	4100	est.[p]
$C_2F_4Cl + O_2 \rightleftarrows CF_2Cl + CF_2{:}O + O$	1.3×10^{13}	0	23000	est.[p]
$C_2F_4Cl + H \rightleftarrows CHF_2 + CF_2Cl$	4.37×10^{16}	−0.746	4360	est.[p]
$C_2F_4Cl + H_2O_2 \rightleftarrows C_2HF_4Cl + HO_2$	9.0×10^{9}	0	1000	est.[p]
$C_2F_4Cl + O \rightleftarrows CF_2Cl + CF{:}O + F$	2.2×10^{13}	0	0	est.[p]
$C_3H_8 + C_2F_4Cl \rightleftarrows n\text{-}C_3H_7 + C_2HF_4Cl$	3.9×10^{11}	0	7800	est.[p]
$C_3H_8 + C_2F_4Cl \rightleftarrows i\text{-}C_3H_7 + C_2HF_4Cl$	3.3×10^{11}	0	6100	est.[p]
$C_2F_4Cl \rightleftarrows CF_2 + CF_2Cl$	4.27×10^{15}	0	56240	est.[p]
$C_2F_4Cl + F \rightleftarrows CF_2Cl + CF_3$	3.16×10^{13}	0	0	est.[p]
$C_2F_4Cl + O \rightleftarrows CF_2{:}O + CF_2Cl$	1.1×10^{13}	0	0	est.[p]
$C_2F_4Cl + OH \rightleftarrows CF_2Cl + CF{:}O + HF$	2.2×10^{13}	0	0	est.[p]
$C_2F_4Cl + HO_2 \rightleftarrows CF_2Cl + CF_2{:}O + OH$	3.0×10^{13}	0	0	est.[p]
$C_2F_4Cl + HO_2 \rightleftarrows C_2HF_4Cl + O_2$	3.0×10^{11}	0	0	est.[p]
$C_2F_4Cl + CH_2O \rightleftarrows C_2HF_4Cl + HCO$	5.5×10^{3}	2.8	5900	est.[p]
$C_2F_4Br + CH_2O \rightleftarrows C_2HF_4Br + HCO$	5.5×10^{3}	2.8	5900	est.[p]
$C_2HF_4Cl \rightleftarrows C_2F_4 + HCl$	4.0×10^{13}	0	71600	est.[q]
$CHF_2 + CF_2Cl \rightleftarrows C_2HF_4Cl$	2.61×10^{26}	−4.16	4100	est.[q]
$C_2HF_4Cl + H \rightleftarrows C_2F_4Cl + H_2$	1.4×10^{7}	1.6	10200	est.[q]
$C_2HF_4Cl + O \rightleftarrows C_2F_4Cl + OH$	7.0×10^{7}	1.6	7200	est.[q]
$C_2HF_4Cl + OH \rightleftarrows C_2F_4Cl + H_2O$	1.4×10^{7}	1.6	2246	est.[q]
$C_2HF_4Cl + CH_3 \rightleftarrows C_2F_4Cl + CH_4$	5.7×10^{10}	0	9500	est.[q]
$C_2HF_4Cl + C_2H_3 \rightleftarrows C_2F_4Cl + C_2H_4$	6.0×10^{10}	0	7000	est.[q]
$C_2HF_4Cl + C_2H_5 \rightleftarrows C_2F_4Cl + C_2H_6$	5.7×10^{10}	0	11800	est.[q]
$C_2HF_4Cl + C_2H_5O \rightleftarrows C_2F_4Cl + C_2H_5OH$	5.7×10^{10}	0	10600	est.[q]
$C_2HF_4Cl + sC_2H_4OH \rightleftarrows C_2F_4Cl + C_2H_5OH$	5.7×10^{10}	0	15900	est.[q]
$C_2HF_4Cl + pC_2H_4OH \rightleftarrows C_2F_4Cl + C_2H_5OH$	5.7×10^{10}	0	8900	est.[q]
$C_2HF_4Cl + CH_2F \rightleftarrows C_2F_4Cl + CH_3F$	2.0×10^{11}	0	10000	est.[q]
$C_2HF_4Cl + CHF_2 \rightleftarrows C_2F_4Cl + CH_2F_2$	2.0×10^{11}	0	10000	est.[q]
$C_2HF_4Cl + CF_3 \rightleftarrows C_2F_4Cl + CHF_3$	1.4×10^{11}	0	10100	est.[q]
$C_2HF_4Cl + Br \rightleftarrows HBr + C_2F_4Cl$	1.1×10^{13}	0	19300	est.[q]
$C_2HF_4Cl + Cl \rightleftarrows HCl + C_2F_4Cl$	1.1×10^{13}	0	29500	est.[q]
$C_2HF_4Cl + F \rightleftarrows C_2F_4Cl + HF$	4.0×10^{13}	0	1400	est.[q]
$C_2HF_4Br \rightleftarrows C_2F_4 + HBr$	4.0×10^{13}	0	71600	est.[q]
$CHF_2 + CF_2Br \rightleftarrows C_2HF_4Br$	2.61×10^{26}	−4.16	4100	est.[q]
$C_2HF_4Br + H \rightleftarrows C_2F_4Br + H_2$	1.4×10^{7}	1.6	10200	est.[q]
$C_2HF_4Br + O \rightleftarrows C_2F_4Br + OH$	7.0×10^{7}	1.6	7200	est.[q]
$C_2HF_4Br + OH \rightleftarrows C_2F_4Br + H_2O$	1.4×10^{7}	1.6	2246	est.[q]
$C_2HF_4Br + CH_3 \rightleftarrows C_2F_4Br + CH_4$	5.7×10^{10}	0	9500	est.[q]
$C_2HF_4Br + C_2H_3 \rightleftarrows C_2F_4Br + C_2H_4$	6.0×10^{10}	0	7000	est.[q]
$C_2HF_4Br + C_2H_5 \rightleftarrows C_2F_4Br + C_2H_6$	5.7×10^{10}	0	11800	est.[q]
$C_2HF_4Br + C_2H_5O \rightleftarrows C_2F_4Br + C_2H_5OH$	5.7×10^{10}	0	10600	est.[q]
$C_2HF_4Br + sC_2H_4OH \rightleftarrows C_2F_4Br + C_2H_5OH$	5.7×10^{10}	0	15900	est.[q]
$C_2HF_4Br + pC_2H_4OH \rightleftarrows C_2F_4Br + C_2H_5OH$	5.7×10^{10}	0	8900	est.[q]
$C_2HF_4Br + CH_2F \rightleftarrows C_2F_4Br + CH_3F$	2.0×10^{11}	0	10000	est.[q]
$C_2HF_4Br + CHF_2 \rightleftarrows C_2F_4Br + CH_2F_2$	2.0×10^{11}	0	10000	est.[q]
$C_2HF_4Br + CF_3 \rightleftarrows C_2F_4Br + CHF_3$	1.4×10^{11}	0	10100	est.[q]
$C_2HF_4Br + Br \rightleftarrows HBr + C_2F_4Br$	1.1×10^{13}	0	19300	est.[q]
$C_2HF_4Br + Cl \rightleftarrows HCl + C_2F_4Br$	1.1×10^{13}	0	29500	est.[q]
$C_2HF_4Br + F \rightleftarrows C_2F_4Br + HF$	4.0×10^{13}	0	1400	est.[q]
$Br + CF_2 + M \rightleftarrows CF_2Br + M$	3.6×10^{17}	0	0	est.[r]

DOI: 10.1021/acs.jpca.5b00959
J. Phys. Chem. A XXXX, XXX, XXX−XXX

Table 2. continued

reaction	A	n	E_a	ref
$C_2H_4 + CF_2Br \rightleftarrows C_2H_3 + CHF_2Br$	1×10^{11}	0	3080	51
$C_2H_3 + Br \rightleftarrows C_2H_3Br$	9.0×10^{13}	0	0	est.[s]
$C_2H_3Cl \rightleftarrows C_2H_3 + Cl$	8.0×10^{15}	0	91600	est.[t]
$C_2H_3Br + Cl \rightleftarrows C_2H_3Cl + Br$	8.61×10^{13}	0	0	52
$C_2H_4 + Cl \rightleftarrows C_2H_3 + HCl$	3.01×10^{11}	0	0	53
$H_2 + Br \rightleftarrows HBr + H$	1.7×10^{14}	0	19200	54

[a]On the basis of reciprocity with CF_3Br reactions. [b]The reaction rate corresponds to a 0.85/0.15 split from the reaction $C_2F_4 + O \rightleftarrows$ products, as observed experimentally in Nguyen et al.[38] [c]The same 0.85/0.15 split was adopted from the measurements from Nguyen et al.[38] for the reaction $C_2F_4 + O \rightleftarrows$ products. [d]On the basis of reciprocity between reactions with CH_3 and C_2H_3. [e]Same rate as the similar reaction with C_2H_5. [f]Same rate as $C_2Cl_5 + Cl \rightleftarrows C_2Cl_4 + Cl_2$. [g]Same rate as $HBr + Cl_2 \rightleftarrows HCl + BrCl$ from Goldfinger et al.[47] [h]Same rate as $BrCl + O \rightleftarrows BrO + Cl$ from Clyne et al.[48] [i]Same rate as $Cl_2 + H \rightleftarrows HCl + Cl$ [j]Same rate as $CF_2Cl + F \rightleftarrows CF_3 + Cl$ [k]On the basis of the rates for similar reactions with CF_2Cl as a reactant with E_a adjusted on the same base as the difference between the reactions involving CF_2BrCl. [l]On the basis of the rates for similar reactions with CHF_2Cl as a reactant with E_a adjusted on the same base as in footnote *k*. [m]On the basis of $CF_2Cl + CF_2Cl \rightleftarrows CF_2Cl_2 + CF_2$. [n]On the basis of $H + CF_2Br_2 \rightleftarrows HBr + CF_2Br$ with reciprocity with CF_2Cl_2 reactions. [o]Same rate as the equivalent reaction with C_2F_6. [p]Same rate as the equivalent reaction with C_2F_5. [q]Same rate as the equivalent reaction with C_2HF_5. [r]Same rate as Cl+ CF_2 + M $\rightleftarrows$ CF_2Cl + M in Codnia and Azcárate.[55] [s]Reaction rate from Babushok et al.[56] multiplied by a factor of 3. [t]Theoretical reaction rate from Manion and Louw[57] multiplied by a factor of 2.

the laminar flame speed. In the case of methane (a), a reduction of the maximum flame speed by a factor higher than 2 was observed. Comparing the Halon 1211 effects with previous results for CF_3Br from Osorio et al.[16] shows that the difference between the two fire suppressants is rather slim, as a difference of only around 0.5 cm/s was observed at ϕ = 1.1 where the laminar flame speed is at its maximum. When Halon 1211 is added to C_2H_4 (b), a noticeable reduction in the laminar flame speed is observed as well. However, this reduction is not as important as for CH_4, since a factor of around 1.7 can be measured between the maximum flame speeds. The comparison with the new CF_3Br data shows that CF_3Br seems to be slightly more efficient at reducing the flame speed under the present conditions. However, the differences in the laminar flame speeds are below 1 cm/s at a given equivalence ratio, which can be considered negligible given the aforementioned experimental uncertainty. Finally, a reduction factor above 1.8 can be observed with the laminar flame speed of C_3H_8. In this case as well, there is basically no difference between the two fire suppressants, except for the fuel-rich case, where CF_2BrCl seems to be slightly less efficient at reducing the flame speed than CF_3Br. However, it should be noted that for the three fuels considered, the difference in the laminar flame speeds between Halon 1301 and Halon 1211 is within the reported experimental uncertainty and can be considered negligible.

4. MODELING

4.1. Model Description. All of the ignition delay time simulations within this study were performed using the CHEMKIN-PRO package from Reaction Design.[31] The computations were made using the Closed Homogeneous Reactor model, along with the Constrain Volume and Solve Energy Equation problem type. The laminar flame speed modeling was performed using the COSILAB[32] software. COSILAB was used over CHEMKIN-PRO to perform the laminar flame speed calculations because of its better ability to converge to a solution with fire-suppressant-containing mixtures.

The tentative model proposed in this study is based on the hydrocarbon model developed by the group of Curran and co-workers for hydrocarbons up to C5[33] and recently updated by Metcalfe et al.[34] (Aramcomech 1.3) for the H_2/C1−C2 part. The Halon 1211 model uses various submodels from the literature as a foundation. These models are the recent $C_3H_2F_3Br$ model of Babushok et al.[12] (which also includes the CF_3Br chemistry), while reactions involving chlorine have been taken from the HCFC-123 ($C_2HCl_2F_3$) model of Babushok et al.[35] As mentioned earlier, the pyrolysis of Halon 1211 with[21] and without[22] H_2 was detailed by Yu et al., and these submechanisms have been used as a starting point to develop the oxidation chemistry of CF_2BrCl. In cases of duplicate reactions, the rates adopted by Babushok and co-workers were kept. It was then necessary to develop the oxidation chemistry of the species defined in the work of Yu et al. until the products of the oxidation steps become the species involved in the mechanisms from Babushok and co-workers.[12,35] Whenever necessary, the thermodynamic properties of species were calculated using the THERGAS package[36] (C_3H_6Cl, *i*-C_3H_7Cl, CF_2Br_2, CF_2BrCl, and C_2F_3Cl) or, for the larger and more complex species (C_2F_4BrCl, C_2HF_4Cl, C_2HF_4Br, C_2F_4Cl and C_2F_4Br), the THERM package.[37] The reactions added or modified during this study to develop the Halon 1211 chemistry are listed in Table 2, and the full mechanism, along with the thermodynamic data calculated for this study, is available in the Supporting Information.

As shown in Table 2, the reactions necessary to complete the Halon 1211 oxidation have been taken from the literature whenever possible. When no reaction rate was available from the literature, the reaction rate was estimated by similarities with existing reactions in the mechanism. In addition to these additions, it was found necessary to change the reaction rate for the reaction $H_2 + Br \rightleftarrows HBr + H$. As will be shown later, this reaction is important and has a different reaction rate in the models of Yu et al.[21] and Babushok et al.[12] However, neither of these two rates led to accurate predictions of the shock-tube results, so the value recommended in the review of Baulch et al.[54] was adopted. In addition, the original computations with the shock-tube data for C_2H_4/Halon 1211 mixtures predicted ignition delay times that were significantly too short. A similar observation was made with C_2H_4 when either CF_3I[23] or CF_3Br (this study) was used as the fire suppressant. This aspect was investigated using sensitivity analysis with the C_2H_4/CF_3Br data, and it was found that the reaction $C_2H_3 + Br \rightleftarrows C_2H_3Br$ seemed to be responsible for the discrepancy between the model and the data. The rate of this reaction was estimated in the earlier work of Babushok et al.,[56] and the reverse reaction was estimated by calculation by Crespo et al.[58] Again, none of these reaction rates was found to be satisfactory, and

DOI: 10.1021/acs.jpca.5b00959
J. Phys. Chem. A XXXX, XXX, XXX−XXX

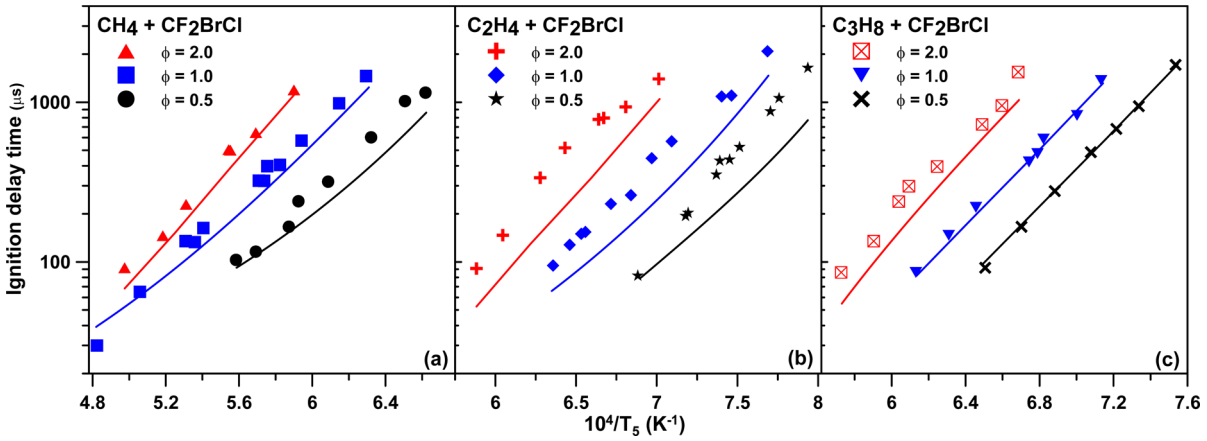

Figure 6. Comparison between the experiments (symbols) and the tentative model (lines) from the present study for the effect of CF_2BrCl on the ignition delay times of (a) CH_4, (b) C_2H_4, and (c) C_3H_8.

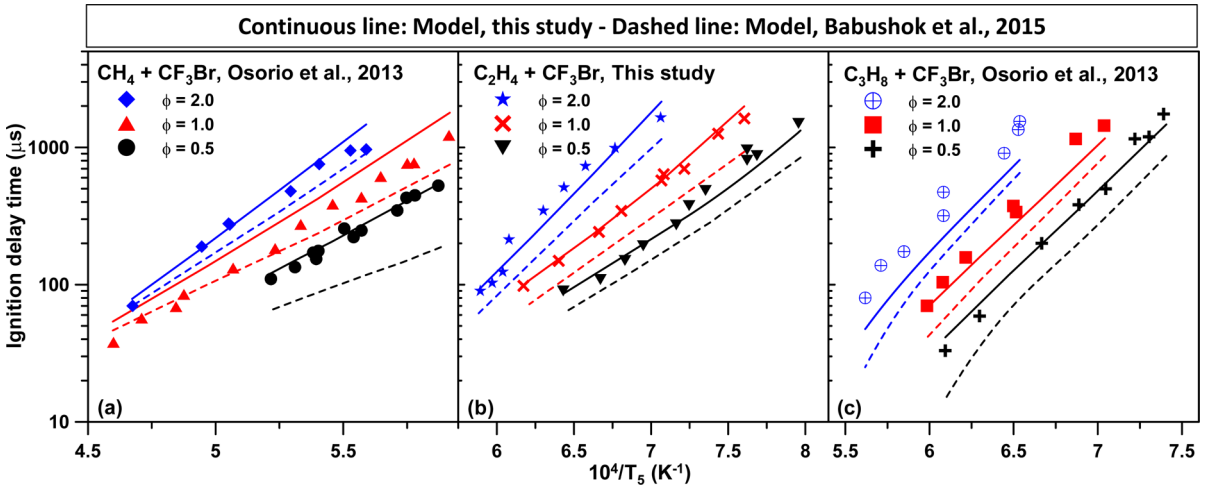

Figure 7. Comparison between models and experimental data for the ignition delay time of (a) CH_4 (Osorio et al.,[16] (b) C_2H_4 (this study), and (c) C_3H_8 (Osorio et al.[16]) with CF_3Br. Continuous lines correspond to the tentative models proposed in the present study, and the dashed lines correspond to the model of Babushok et al.[12]

multiplying the reaction rate estimated by Babushok and coworkers by a factor of 3 allowed the computed predictions to be in satisfactory agreement with the data. This modification also notably improved the predictions of the C_2H_4/CF_2BrCl data.

However, it was also found necessary to revise some reactions involving chlorine atoms. A sensitivity analysis with C_2H_4/CF_2BrCl mixtures showed that out of the 30 most important reactions, only two involved chlorine atoms: $C_2H_3Cl \rightleftarrows C_2H_3 + Cl$ and $C_2H_4 + Cl \rightleftarrows C_2H_3 + HCl$. Better agreement with the data was obtained when the rate of the reaction $C_2H_3Cl \rightleftarrows C_2H_3 + Cl$ from Manion and Louw[57] was multiplied by a factor of 2 and when the rate determined by Dobis and Benson[53] was used for the reaction $C_2H_4 + Cl \rightleftarrows C_2H_3 + HCl$. More details on these modifications are provided in the discussion below, but it should be noted here that these modifications of the interactions between C_2H_4 and halogenated species affected only marginally, if at all, the predictions with CH_4 and C_3H_8.

4.2. Comparison between the Model and the Data. *4.2.1. Shock-Tube Data. Data for CF_2BrCl.* The comparison between the experimental ignition delay time results for hydrocarbons with Halon 1211 obtained during this study and the tentative model are compared in Figure 6 for (a) methane, (b) ethylene, and (c) propane. As can be seen, the data for saturated hydrocarbons (i.e., CH_4 and C_3H_8) are well-reproduced by the model overall. The results for fuel-rich and stoichiometric conditions are predicted within 25% for methane (Figure 6a), except for the highest temperature investigated at $\phi = 1$. The high-temperature data were accurately predicted for the fuel-lean case with CH_4, but a difference of slightly more than 30% between the predicted ignition delay times and the experimental values can be observed below 1685 K. For propane (Figure 6c), the fuel-lean and stoichiometric cases are accurately reproduced over the entire range of temperatures investigated, while the fuel-rich data are predicted within 40%. The predictions for C_2H_4 are, in comparison, less accurate. At $\phi = 0.5$, the data at high temperature are accurately reproduced, but a factor of 2 difference between the model and the experiment is observed on the low-temperature side. Under stoichiometric conditions, the model underpredicts the ignition delay time by around 45% on the low- and high-temperature sides, but factors of up to 2 are observed for the intermediate temperatures as the predictions present a slight curvature.

Finally, the model also underpredicts the data under fuel-rich conditions by between 35% (low temperature) and 45% (high temperature). As discussed later, the interactions between C_2H_4

DOI: 10.1021/acs.jpca.5b00959
J. Phys. Chem. A XXXX, XXX, XXX−XXX

and CF_3Br are well-reproduced by the tentative model. The discrepancy between the experimental results and the Halon 1211 mechanism can therefore be associated with the interactions between chlorine-containing species and the H_2/C_2H_4 chemistry. As mentioned earlier, sensitivity analysis showed that only two reactions involving Cl atoms are important: $C_2H_3Cl \rightleftarrows C_2H_3 + Cl$ and $C_2H_4 + Cl \rightleftarrows C_2H_3 + HCl$. Compared with the original model of Babushok et al., these two reactions have been revised to improve the results. Again, these modifications have little or no effect on the predictions for CH_4 and C_3H_8.

Data for CF_3Br. As mentioned earlier, the tentative CF_2BrCl mechanism is based on the CF_3CHCl_2 and $C_3H_2F_3Br$ chemistry developed by Babushok et al.[12,35] (with the $C_3H_2F_3Br$ mechanism containing the CF_3Br chemistry developed earlier by Noto et al.[59]). Since an important reaction rate involving Br was changed during the present study ($H_2 + Br \rightleftarrows HBr + H$), it was necessary to compare the performance of the tentative model and the original model of Babushok et al.[12] with former results from Osorio et al.[16] This comparison allows an assessment of the impact of this modification on the model's performance with CF_3Br data. Figure 7 presents this comparison between the models and the shock-tube data from Osorio et al. for CF_3Br addition to CH_4 (a) and C_3H_8 (c), along with the C_2H_4 data from this study (b). It should be noted that since the model of Babushok et al. does not contain an OH* submechanism, the OH* mechanism from Hall and Petersen[60] was added so the computed profiles can be compared with the experimental signals. As can be seen, the tentative model is generally in closer agreement with the data than the model of Babushok and co-workers.[12] With methane (a), the model of Babushok et al. predicts ignition delay times that are factors of around 2 and 3 shorter than the experimental values for the fuel-lean case. Under these conditions, the tentative model predicts the data with high accuracy. For the stoichiometric case, the activation energies derived from the experimental data (51.2 kcal/mol) and the model (52.8 kcal/mol) are similar, but the model overpredicts the ignition delay time by a factor of around 1.45. In comparison, the model of Babushok and co-workers is relatively accurate above 1900 K. Below this temperature, however, the model underpredicts the ignition delay time by factors of up to 1.6. Under the fuel-rich conditions, the tentative model is relatively accurate, whereas the model from the literature tends to be slightly over-reactive.

In regard to propane (Figure 7c), the model proposed in the present study is consistently closer to the experimental data than the model from the literature. The fuel-lean data are accurately reproduced, while the predicted ignition delay times for the stoichiometric and fuel-rich mixtures are too short, with the difference between the model and the data increasing with the equivalence ratio up to a factor of around 1.5. In comparison, the model of Babushok et al. predicts ignition delay times that are too short by a factor of around 2 for all the equivalence ratios investigated.

For the new data with C_2H_4 and CF_3Br (Figure 7b), the model proposed in the present study predicts the ignition delay time data with high accuracy (within 25%) over the range of conditions investigated. By comparison, the model of Babushok et al.[12] presents predicted ignition delay times that are too short by factors between 1.4 (high-temperature side) and 1.8 (low-temperature side) under the conditions investigated.

These comparisons illustrate the improvements induced by the modifications in the reaction rates for $C_2H_3 + Br \rightleftarrows C_2H_3Br$ and $H_2 + Br \rightleftarrows HBr + H$, with the difference between the hydrocarbon mechanisms being relatively small in terms of τ_{ign} predictions, as can be seen in Mathieu et al.[23] However, it should be noted that the kind of results obtained in this study (global kinetics data) are not sufficient to derive or estimate individual reaction rates from such a complex chemical scheme, especially since the rates of many reactions within the fire suppressant mechanisms have only been estimated. Therefore, the changes in the reaction rates used during this study for reactions involving species containing Br and Cl should only be used as indications pointing to a need for more accurate measurements. In particular, one can therefore conclude from this study with CF_3Br and CF_2BrCl and a recent study by our group with CF_3I that interactions between C_2H_4 (and probably other unsaturated hydrocarbon molecules) and halogens need to be revisited.

4.2.2. Laminar Flame Speed Data. The laminar flame speed data for the neat hydrocarbons and the hydrocarbons with addition of CF_3Br or CF_2BrCl were modeled with the tentative mechanism and with the model of Babushok et al.[12] (for the neat and CF_3Br addition data only). The comparison between the models and the laminar flame speed data is visible in Figure 5 for (a) methane, (b) ethylene, and (c) propane. With methane, the model predicts laminar flame speeds that are higher than the experimental results. This overprediction is rather small with neat methane (5−25% difference between the tentative model and the data and 20−30% difference for the model of Babushok et al.) but is more noticeable for the CF_2BrCl addition. In this case, the laminar flame speed is overpredicted by factors of 1.4 (fuel-lean to stoichiometric) to 1.75 (fuel-rich side). For the CF_3Br addition, the two models yield nearly the same results, with the mechanism of Babushok et al.[12] being slightly closer to the data, especially on the fuel-rich side. However, it should be noted that the difference between the models is rather small (less than 1 cm/s at ϕ = 1.2). Overall, compared with the experimental data for CF_3Br, both mechanisms overpredict the laminar flame speed by a factor of around 1.5.

With neat ethylene (Figure 5b), the model of Metcalfe et al.[34] used in this study also tends to slightly overestimate the data, notably on the fuel-rich side, where a difference of 10−15% between the model and the data can be observed. A relatively large difference (around 5 cm/s) can be seen for the maximum laminar flame speeds predicted by this mechanism and the mechanism of Babushok et al., which underestimates this maximum value but is relatively accurate on the fuel-lean and fuel-rich sides. As for methane, the laminar flame speeds upon CF_2BrCl addition are largely overpredicted by the tentative model, by factors ranging from around 1.1 on the fuel-lean side to around 1.4 on the fuel-rich side. The predictions for the Halon 1301 addition are more accurately reproduced by the models, and the laminar flame speed is adequately predicted below ϕ = 1. Above this equivalence ratio, however, the computed laminar flame speeds are too high, by up to around 10% with the model of Babushok et al. and around 15% with the tentative model. It should be noted that the difference between the models of Babushok et al. and the present study can be due to the difference between the two models for the neat ethylene mixture.

With propane (Figure 5c), the laminar flame speed for the neat mixture is slightly overpredicted under fuel-lean conditions but is then underpredicted for equivalence ratios above 1.1, with the two models being in close agreement (the model of

DOI: 10.1021/acs.jpca.5b00959
J. Phys. Chem. A XXXX, XXX, XXX−XXX

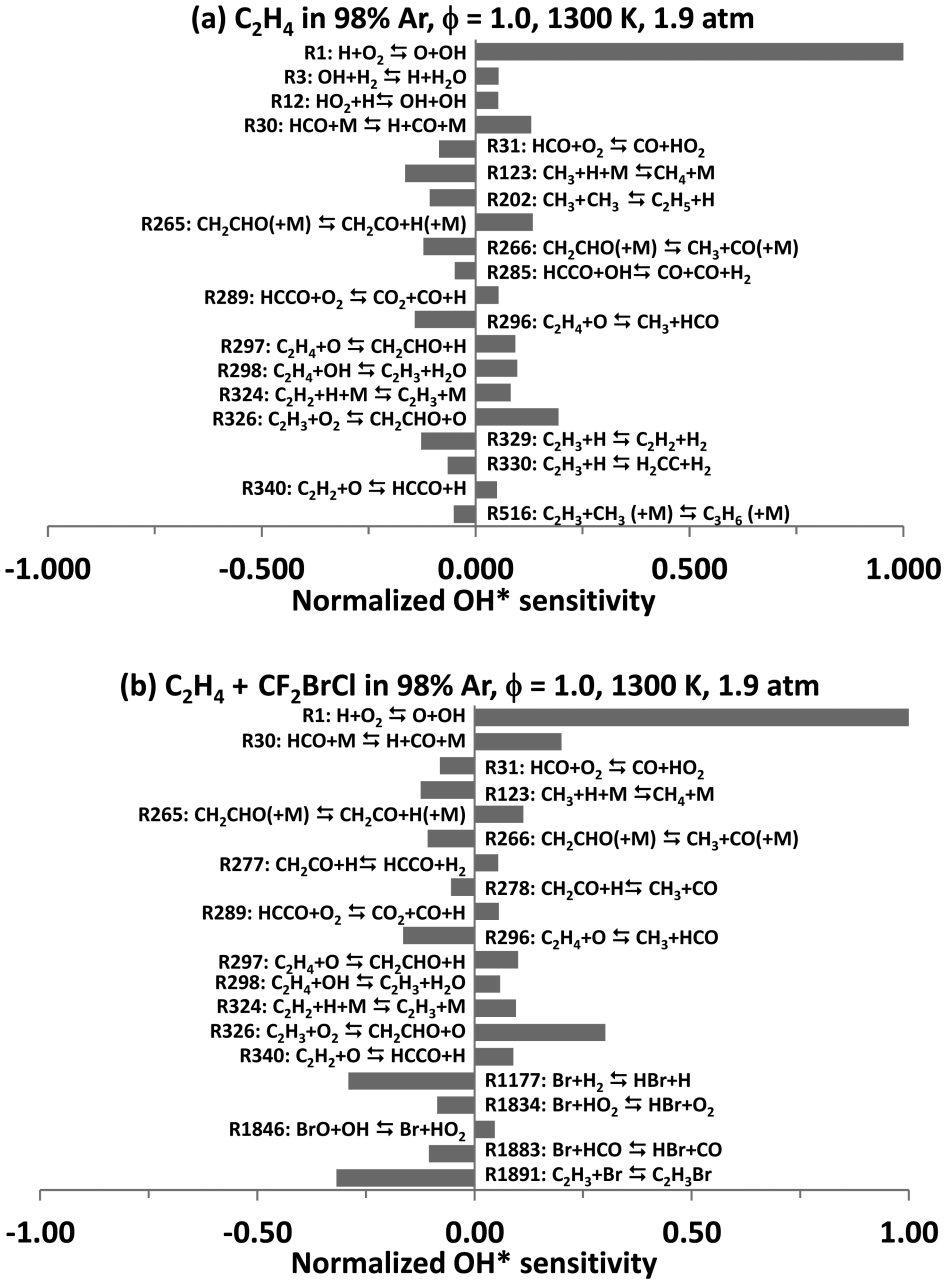

Figure 8. Normalized sensitivity analysis on OH* for stoichiometric mixtures of (a) C_2H_4 and (b) C_2H_4 with CF_2BrCl in Ar at 1300 K and 1.9 atm. A positive sensitivity coefficient indicates a reaction that promotes the reactivity of the mixture (i.e., reduces the ignition delay time). A negative sensitivity coefficient indicates a reaction that inhibits the reactivity.

Babushok et al. predicting a slightly higher laminar flame speed by 2% or less). When CF_2BrCl is added to mixture, the calculated laminar flame speed is still largely overpredicted. However, the calculated flame speed is closer to the data than for CH_4, as factors between 1.3 (fuel-lean) and 1.2 (fuel-rich) can be observed. As for the other hydrocarbons investigated, the CF_3Br/propane data are better predicted by the models. With propane, the two models yield nearly the same result, and the computed laminar flame speeds are too long by a factor of around 1.1.

5. Chemical Analysis. A sensitivity analysis on OH* was conducted for each mixture investigated in the shock tube on both the high- and low-temperature sides of the curves. From a comparison of the sensitivity analyses for the neat mixture and the mixture with CF_2BrCl addition under similar conditions, the important reactions involving Halon 1211 and its effect on the ignition delay time can be determined. An example of these sensitivity analyses is provided in Figure 8 for ethylene at 1300 K and ϕ = 1.0. In this figure, the sensitivities were normalized to the highest value, and a positive sensitivity coefficient (σ) indicates a reaction that promotes the reactivity of the mixture (i.e., reduces the ignition delay time). Conversely, a negative σ indicates a reaction that inhibits the reactivity. In the following discussion, the reaction numbers listed refer to the positions of the corresponding reactions in the mechanism.

As can be seen in this figure, the addition of Halon 1211 (Figure 8b) leads to the appearance of several reactions involving radicals and atoms containing Br. The most sensitive reaction,

DOI: 10.1021/acs.jpca.5b00959
J. Phys. Chem. A XXXX, XXX, XXX−XXX

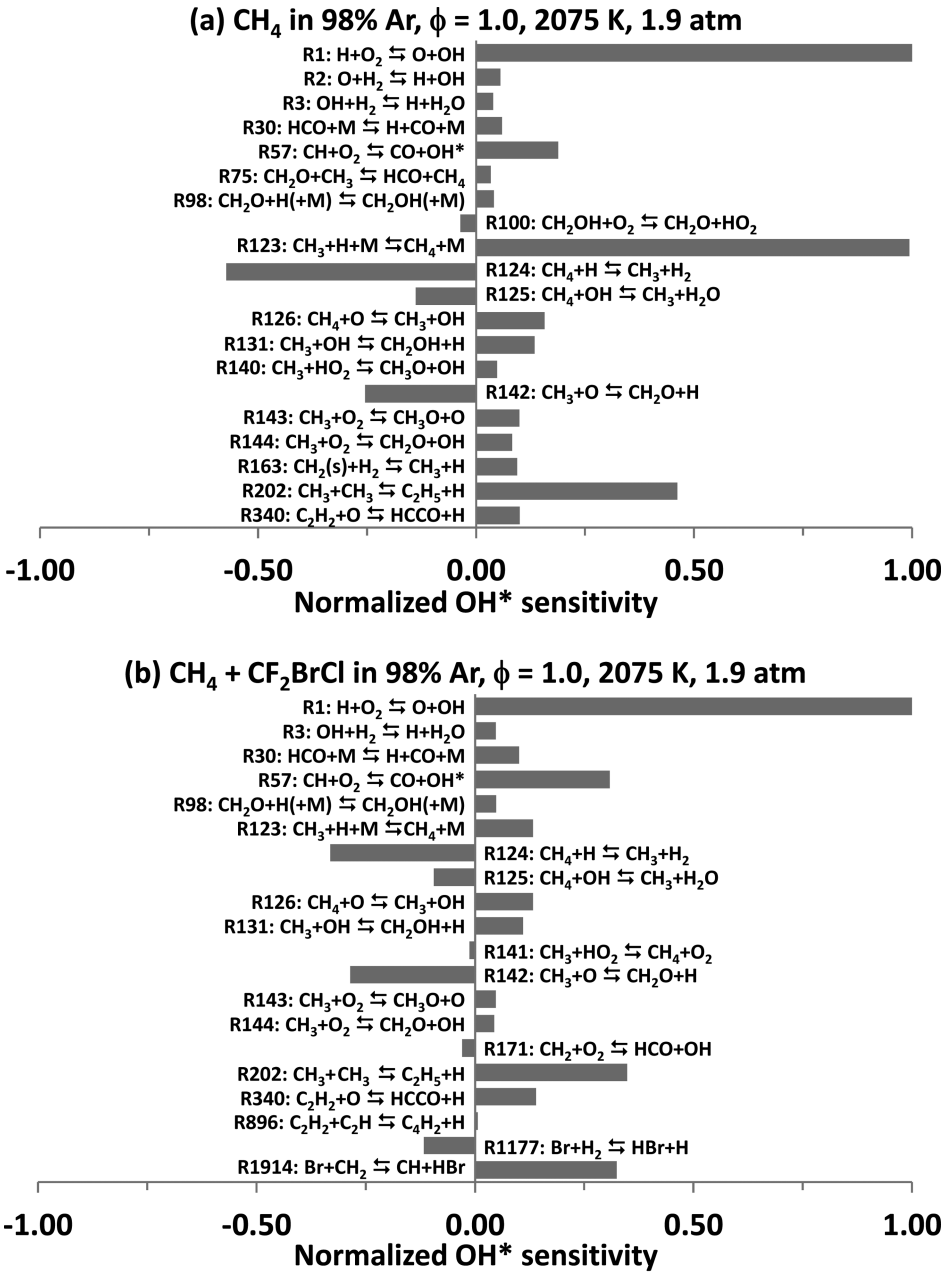

Figure 9. Normalized sensitivity analysis on OH* for stoichiometric mixtures of (a) CH_4 and (b) CH_4 with CF_2BrCl in Ar at 2075 K and 1.9 atm. A positive sensitivity coefficient indicates a reaction that promotes the reactivity of the mixture (i.e., reduces the ignition delay time). A negative sensitivity coefficient indicates a reaction that inhibits the reactivity.

$$H + O_2 \rightleftarrows O + OH \quad \text{(R1)}$$

is the same for the two mixtures, and one can see that most of the reactions that do not involve the fire suppressant are the same. In most cases, the reactions involving Br atoms inhibit reactions (through radical termination), and two of them have significant sensitivity coefficients:

$$Br + H_2 \rightleftarrows HBr + H \text{ (in reverse)} \quad \text{(R1177)}$$

and

$$C_2H_3 + Br \rightleftarrows C_2H_3Br \quad \text{(R1891)}$$

Reaction R1891 inhibits the reactivity of the vinyl radical, while reaction R1177 consumes a hydrogen radical that will then not be able to react through the branching reaction R1. The other inhibiting reactions are terminating reactions of combustion radicals, such as

$$Br + HO_2 \rightleftarrows HBr + O_2 \quad \text{(R1834)}$$

and

$$Br + HCO \rightleftarrows HBr + CO \quad \text{(R1883)}$$

It should be noted that equilibrium calculations showed HBr to be the final product after the combustion of the mixtures investigated under the conditions of this study with CF_2BrCl.

At a higher temperature of 1575 K (results not shown), similar reactions involving Br atoms are found, but reactions involving Cl atoms are also present. These reactions are

$$Cl + C_2H_4 \rightleftarrows C_2H_3 + HCl \quad \text{(R1940)}$$

DOI: 10.1021/acs.jpca.5b00959
J. Phys. Chem. A XXXX, XXX, XXX−XXX

Table 3. Catalytic Cycles Involving Bromine Species, Adapted from CF_3Br to CF_2BrCl for Cycle III

cycle I[56]	cycle II[61]	cycle III[62,63]	cycle IV[64]
	$H + HBr \rightleftarrows H_2 + Br$	$H + CF_2BrCl \rightleftarrows CF_2Cl + HBr$	
$H + HBr \rightleftarrows H_2 + Br$	$H + CH_3Br \rightleftarrows HBr + CH_3$	$H + HBr \rightleftarrows H_2 + Br$	$CH_3 + HBr \rightleftarrows CH_4 + Br$
$H + Br_2 \rightleftarrows HBr + Br$	$CH_3 + Br_2 \rightleftarrows CH_3Br + Br$	$CF_2Cl + Br_2 \rightleftarrows CF_2BrCl + Br$	$CH_3 + Br \rightleftarrows CH_3Br$
$Br + Br + M \rightleftarrows Br_2 + M$	$Br + Br + M \rightleftarrows Br_2 + M$	$Br + Br + M \rightleftarrows Br_2 + M$	$CH_3Br + H \rightleftarrows HBr + CH_3$
net: $H + H \rightleftarrows H_2$	net: $H + H \rightleftarrows H_2$	net: $H + H \rightleftarrows H_2$	net: $CH_3 + H \rightleftarrows CH_4$

with $\sigma = 0.06$ and

$$C_2H_3Cl \rightleftarrows C_2H_3 + Cl \text{ (in reverse)} \quad \text{(R2190)}$$

with $\sigma = -0.08$. The two reactions involving Cl atoms therefore have low sensitivity coefficients and almost cancel each other in terms of their effects on the overall reactivity.

With C_3H_8 mixtures (results not shown), reaction R1177 is the only reaction among the 20 most sensitive ones that involves an atom coming from Halon 1211 at high temperature (1630 K). The sensitivity coefficient is relatively small ($\sigma = -0.08$), which is in agreement with the experimental results, where the effect of CF_2BrCl addition is rather modest at high temperature with C_3H_8 (Figure 4). At lower temperature (1400 K), where the effect of Halon 1211 is more important, reaction R1177 has a higher sensitivity ($\sigma = -0.19$, the third most-important sensitivity), and two other reactions involving Br atoms are also participating, reactions R1891 and R1924 ($C_3H_8 + Br \rightleftarrows i\text{-}C_3H_7 + HBr$, in reverse), both with a modest sensitivity coefficient of −0.06.

For the methane case, the reactivity was notably increased by the Halon 1211 addition. The reactivity was also increased by the additions of Halon 1301 and Halon 13001, but in smaller proportions (see Figure 2). For the CF_3Br and CF_3I cases, the reduction in the ignition delay time was associated with the following branching reaction:[16,23]

$$CF_3 + O_2 \rightleftarrows CF_3O + O \quad \text{(R1264)}$$

where the resulting O radical then promotes the reactivity essentially via

$$O + H_2 \rightleftarrows OH + H \quad \text{(R2)}$$

and also via

$$O + CH_4 \rightleftarrows OH + CH_3 \quad \text{(R126)}$$

Since there is no CF_3 group in CF_2BrCl, reaction R1264 cannot be directly associated with the large increase in the reactivity for methane ignition. A sensitivity analysis on OH* was also performed with methane (Figure 9), and this analysis also lists reaction R1177 with a sensitivity coefficient that is not negligible ($\sigma = -0.12$), but the other reaction involving Halon 1211-related species is

$$Br + CH_2 \rightleftarrows CH + HBr \quad \text{(R1914)}$$

which has the second-largest sensitivity coefficient ($\sigma = 0.32$) after reaction R1. The resulting CH radical can then react with O_2 or radicals to promote the reactivity via

$$CH + O_2 \rightleftarrows HCO + O \quad \text{(R176)}$$

$$CH + O \rightleftarrows CO + H \quad \text{(R180)}$$

$$CH + OH \rightleftarrows HCO + H \quad \text{(R181)}$$

Additionally, it is worth mentioning that the main formation pathway for OH* during combustion of hydrocarbons is

$$CH + O_2 \rightleftarrows CO + OH^* \quad \text{(R57)}$$

The presence of Br radicals therefore seems to enhance the formation of the OH* radicals, whose chemiluminescence was used to determine the ignition delay time in our experiments. To illustrate this effect, one can see that when Halon 1211 is added to the mixture, the sensitivity of reaction R57 increases from 0.19 (Figure 9a, neat mixture) to 0.31 (Figure 9b, mixture with CF_2BrCl).

However, despite the high sensitivity coefficient of reaction R1914 with respect to OH* under our conditions and although the aforementioned subsequent reactions of CH radical with O, O_2, and OH (reactions R176, R180, and R181; see above) promote the reactivity of the mixture, this pathway is not important enough to explain the large increase in the reactivity when CF_2BrCl is added to the CH_4 mixture. A further investigation was then performed with reaction pathway analysis, and this analysis showed that the reaction

$$CH_3 + CF_2 \rightleftarrows CH_2{:}CF_2 + H \quad \text{(R1740)}$$

plays an important role in producing H radicals in the early stage of the reactivity. These H radical can then react with O_2 through reaction R1, which is the most sensitive promoting reaction under the present conditions.

This result also explains the noticeably larger increase in the reactivity observed with CF_2BrCl addition compared with CF_3Br or CF_3I addition to CH_4 mixtures (see Figure 2). Indeed, as mentioned above, CF_3Br and CF_3I increase the reactivity through reaction R1264, and the O radicals produced then react via the promoting reactions R2 and R126. On the other hand, CF_2BrCl promotes reaction R1 via the formation of H radicals through reaction R1740, and reaction R1 promotes the reactivity in larger proportions than reactions R2 and R126 under the present conditions.

To summarize, under the conditions of the present study, the presence of Halon 1211 in a mixture containing methane promotes (i) the formation of OH* (as shown by the sensitivity analysis with R1914 followed by R57) and (ii) the reactivity of the mixture by converting CH_3 radicals into reactive H radicals via reaction R1740, thereby promoting the important branching reaction R1.

It is therefore interesting to conclude from these chemical analyses that Halon 1211 essentially reduces the reactivity of C_2H_4 and C_3H_8 via the consumption of H radicals by HBr (reaction R1177), thereby inhibiting the promoting reaction R1, whereas Halon 1211 enhances the reactivity of CH_4 by promoting this same reaction R1 via reaction R1740.

For the laminar flame speed case, results are more consistent, as relatively large reductions in the laminar flame speed were observed for all of the fuels. The sensitivity analysis with the shock-tube results stressed the importance of Br over Cl atoms in the chemical effect of Halon 1211 on the combustion properties. The effect of Br in Halon 1211 on the flame speed is the same as with CF_3Br, which has been described in the

DOI: 10.1021/acs.jpca.5b00959
J. Phys. Chem. A XXXX, XXX, XXX−XXX

literature. Four catalytic cycles have been identified for CF_3Br,[16] and those catalytic cycles would correspond to the cycles described in Table 3 for CF_2BrCl.

It should be noted that although the Cl atom seems significantly less efficient than Br at inhibiting oxidation, similar cycles could be imagined by replacing Br and Cl by each other in Table 3. Moreover, it is also worth mentioning that the tentative model from the present study yields results that vary significantly between CF_3Br and CF_2BrCl. This difference between the two suppressants indicates the need for further study of the interactions between the CF_2 group and hydrocarbons and, more importantly, the interactions between the chlorine atom and hydrocarbons during combustion.

6. CONCLUSIONS

In this study, the effect of Halon 1211 on the ignition delay times and laminar flame speeds of methane, ethylene, and propane was investigated experimentally for the first time. The results showed a large decrease in the laminar flame speed for all three fuels, with results nearly identical to those for CF_3Br from previous studies. The shock-tube results showed a decrease in the reactivity with propane and ethylene, whereas a large decrease in the ignition delay time of methane was observed with CF_2BrCl addition. A tentative mechanism was assembled from submechanisms and reactions from the literature along with estimations based on similarities of several individual reactions. The tentative model gave good results in predicting the shock-tube data, including former and new data with CF_3Br. On the other hand, laminar flame speeds were overpredicted by factors between 1.1 and 1.75 for the Halon 1211 data and by smaller factors for Halon 1301. The computed values for CF_3Br are comparable to the performance of existing mechanisms in the literature for CF_3Br, and the fire suppressant effects can be attributed to catalytic cycles involving bromine atoms and, to a much lesser extent, chlorine atoms.

Sensitivity and reaction pathway analyses showed the prominent role of the bromine atom in the shock-tube results with C_2H_4 and C_3H_8, whereas the CF_2 radical plays a major role with CH_4. With propane and ethylene, the effect of Halon 1211 on the ignition delay time is essentially due to the consumption of H radicals through the reaction HBr + H ⇄ Br + H_2 (R1177), which then inhibits the branching reaction H + O_2 ⇄ OH + O (R1). In the case of methane, CF_2 radicals promote the formation of H radicals by reacting with CH_3 (CH_3 + CF_2 ⇄ CH_2:CF_2 + H, reaction R1740). These H radicals then react with O_2 and promote the reactivity through the branching reaction R1.

Overall, it was found that the tentative mechanism proposed in this study predicts with reasonable to high accuracy the ignition delay times for the light hydrocarbons investigated herein with both CF_3Br and CF_2BrCl. More work is required to improve the laminar flame speed predictions, and this study exhibits the need for a better understanding of the interactions between chlorine atoms and hydrocarbons during combustion. Direct measurements of key rates are needed for many of the reactions of importance to the fire suppressant chemistry, since many of the rate coefficients currently are only estimates.

■ ASSOCIATED CONTENT

Supporting Information

Ignition delay times (Table S1), laminar flame speeds (Table S2), and text files containing the full kinetic mechanism and the thermodynamic data. This material is available free of charge via the Internet at http://pubs.acs.org.

■ AUTHOR INFORMATION

Corresponding Author

*E-mail: epetersen@tamu.edu.

Notes

The authors declare no competing financial interest.

■ ACKNOWLEDGMENTS

The authors acknowledge Dr. Pierre-Alexandre Glaude for his help with the THERGAS software as well as Dr. Joseph Bozzelli for his help with the THERM software and for the calculations of the NASA polynomials for a few species. Dr. Nabiha Chaumeix and Dr. Valeri Babushok are also thanked for help with the laminar flame speed calculations using the COSILAB software and for the helpful discussions on fire suppressant chemistry, respectively. During this study, C.G. was a visiting researcher at Texas A&M University from Université d'Orléans, France.

■ REFERENCES

(1) Anderson, J. G.; Brune, W. H.; Lloyd, S. A.; Toohey, D. W.; Sander, S. P.; Starr, W. L.; Loewenstein, M.; Podolske, J. R. Kinetics of O_3 destruction by ClO and BrO within the Antarctic vortex: An analysis based on in situ ER-2 data. *J. Geophys. Res.: Atmos.* **1989**, *94*, 11480−11520.

(2) Salawitch, R. J.; Wofsy, S. C.; Gottlieb, E. W.; Lait, L. R.; Newman, P. A.; Schoeberl, M. R.; Loewenstein, M.; Podolske, J. R.; Strahan, S. E. Chemical loss of ozone in the Arctic polar vortex in the winter of 1991−92. *Science* **1993**, *261*, 1146−1149.

(3) *Montreal Protocol on Substances That Deplete the Ozone Layer, Final Act*; United Nations Environmental Program (UNEP): Montreal, Canada, 1987.

(4) Fraser, P. J.; Oram, D. E.; Reeves, C. E.; Penkett, S. A.; McCulloch, A. Southern hemispheric halon trends (1978−1998) and global halon emissions. *J. Geophys. Res.: Atmos.* **1999**, *104*, 15985−15999.

(5) Montzka, S. A.; Butler, J. H.; Elkins, J. W.; Thompson, T. M.; Clarke, A. D.; Lock, L. T. Present and future trends in the atmospheric burden of ozone-depleting halogens. *Nature* **1999**, *398*, 690−694.

(6) United Nations Environment Program. The Montreal Protocol on Substances That Deplete the Ozone Layer. http://ozone.unep.org/new_site/en/montreal_protocol.php (accessed Mar 3, 2015).

(7) Gann, R. G. Guidance for advanced fire suppression in aircraft. *Fire Technol.* **2008**, *44*, 263−282.

(8) Zhang, S.; Colket, M. B. Modeling cup-burner minimum extinguishing concentration of halogenated agents. *Proc. Combust. Inst.* **2011**, *33*, 2497−2504.

(9) Babushok, V. I.; Linteris, G. T.; Meier, O. C. Combustion properties of halogenated fire suppressants. *Combust. Flame* **2012**, *159*, 3569−3575.

(10) Takahashi, F.; Katta, V. R.; Linteris, G. T.; Meier, O. C. Cup-burner flame structure and extinguishment by CF_3Br and C_2HF_5 in microgravity. *Proc. Combust. Inst.* **2013**, *34*, 2707−2717.

(11) Takahashi, F.; Katta, V. R.; Linteris, G. T.; Babushok, V. I. Combustion inhibition and enhancement of cup-burner flames by CF_3Br, C_2HF_5, $C_2HF_3Cl_2$, and $C_3H_2F_3Br$. *Proc. Combust. Inst.* **2015**, *35*, 2741−2748.

(12) Babushok, V. I.; Linteris, G. T.; Burgess, D. R., Jr.; Baker, P. T. Hydrocarbon flame inhibition by $C_3H_2F_3Br$ (2-BTP). *Combust. Flame* **2015**, *162*, 1104−1112.

(13) Han, W.; Kennedy, E. M.; Mackie, J. C.; Dlugogorski, B. Z. Conversion of CHF_3 to $CH_2{=}CF_2$ via reaction with CH_4 in the presence of $CBrF_3$: An experimental and kinetic modelling study. *J. Hazard. Mater.* **2010**, *180*, 181−187.

DOI: 10.1021/acs.jpca.5b00959
J. Phys. Chem. A XXXX, XXX, XXX−XXX

(14) Linteris, G. T.; Takahashi, F.; Katta, V. R. Cup-burner flame extinguishment by CF_3Br and Br_2. *Combust. Flame* **2007**, *149*, 91−103.
(15) Andersson, B.; Blomqvist, P. Experimental study of thermal breakdown products from halogenated extinguishing agents. *Fire Saf. J.* **2011**, *46*, 104−115.
(16) Osorio, C. H.; Vissotski, A. J.; Petersen, E. L.; Mannan, M. S. Effect of CF_3Br on C_1−C_3 ignition and laminar flame speed: Numerical and experimental evaluation. *Combust. Flame* **2013**, *160*, 1044−1059.
(17) Miller, D. R.; Evers, R. L.; Skinner, G. B. Effects of various inhibitors on hydrogen-air flame speeds. *Combust. Flame* **1963**, *7*, 137−142.
(18) Bajpai, S. N. An investigation of the extinction of diffusion flames by halons. *J. Fire Flammability* **1974**, *5*, 255−267.
(19) Zegers, E. J. P.; Williams, B. A.; Fisher, E. M.; Fleming, J. W.; Sheinson, R. S. Suppression of nonpremixed flames by fluorinated ethanes and propanes. *Combust. Flame* **2000**, *121*, 471−487.
(20) Lemahieu, J.; Antonik, S. Oxidation and combustion of *n*-butane in the presence of bromochlorodifluoromethane. *Bull. Soc. Chim. Fr.* **1982**, *11*−*12* (Part. 1), 413−419.
(21) Yu, H.; Kennedy, E. M.; Azhar Uddin, M. D.; Sullivan, S. P.; Dlugogorski, B. Z. Experimental and computational studies of the gas-phase reaction of Halon 1211 with hydrogen. *Environ. Sci. Technol.* **2005**, *39*, 3020−3028.
(22) Yu, H.; Kennedy, E. M.; Azhar Uddin, M. D.; Sullivan, S. P.; Dlugogorski, B. Z. Experimental and computational studies of the thermal decomposition of Halon 1211. *Int. J. Chem. Kinet.* **2005**, *37*, 134−146.
(23) Mathieu, O.; Goulier, J.; Gourmel, F.; Mannan, M. S.; Chaumeix, N.; Petersen, E. L. Experimental study of the effect of CF_3I addition on the ignition delay time and laminar flame speed of methane, ethylene, and propane. *Proc. Combust. Inst.* **2015**, *35*, 2731−2739.
(24) Aul, C. J.; Metcalfe, W. K.; Burke, S. M.; Curran, H. J.; Petersen, E. L. Ignition and kinetic modeling of methane and ethane fuel blends with oxygen: A design of experiments approach. *Combust. Flame* **2013**, *160*, 1153−1167.
(25) Petersen, E. L.; Rickard, M. J. A.; Crofton, M. W.; Abbey, E. D.; Traum, M. J.; Kalitan, M. D. A facility for gas- and condensed-phase measurements behind shock waves. *Meas. Sci. Technol.* **2005**, *16*, 1716−1729.
(26) Krejci, M. C.; Mathieu, O.; Vissotski, A. J.; Ravi, S.; Sikes, T. G.; Petersen, E. L.; Kéromnès, A.; Metcalfe, W.; Curran, H. J. Laminar flame speed and ignition delay time data for the kinetic modeling of hydrogen and syngas fuel blends. *J. Eng. Gas Turbines Power* **2013**, *135* (2), No. 021503.
(27) de Vries, J.; Lowry, W. B.; Serinyel, Z.; Curran, H. J.; Petersen, E. L. Laminar flame speed measurements of dimethyl ether in air at pressures up to 10 atm. *Fuel* **2011**, *90*, 331−338.
(28) Burke, M. P.; Chen, Z.; Ju, Y.; Dryer, F. L. Effect of cylindrical confinement on the determination of laminar flame speeds using outwardly propagating flames. *Combust. Flame* **2009**, *156*, 771−779.
(29) Chen, Z. On the extraction of laminar flame speed and Markstein length from outwardly propagating spherical flames. *Combust. Flame* **2011**, *158*, 291−300.
(30) Ravi, S.; Sikes, T. G.; Morones, A.; Keesee, C. L.; Petersen, E. L. Comparative study on the laminar flame speed enhancement of methane with ethane and ethylene addition. *Proc. Combust. Inst.* **2015**, *35*, 679−686.
(31) *CHEMKIN-PRO*, version 15131; Reaction Design: San Diego, CA, 2014.
(32) *COSILAB: The Combustion Simulation Laboratory*, version 3.3.2; Rotexo GmbH & Co. KG: Bochum, Germany, 2009; http://www.rotexo.com.
(33) Healy, D.; Kalitan, D. M.; Aul, C. J.; Petersen, E. L.; Bourque, G.; Curran, H. J. Oxidation of C1-C5 alkane quinternary natural gas mixtures at high pressures. *Energy Fuels* **2010**, *24* (3), 1521−1528.
(34) Metcalfe, W. K.; Burke, S. M.; Ahmed, S. S.; Curran, H. J. A hierarchical and comparative kinetic modeling study of C1 − C2 hydrocarbon and oxygenated fuels. *Int. J. Chem. Kinet.* **2013**, *45*, 638−675.
(35) Babushok, V. I.; Linteris, G. T.; Meier, O. C.; Pagliaro, J. L. Flame inhibition by CF_3CHCl_2 (HCFC-123). *Combust. Sci. Technol.* **2014**, *186*, 792−814.
(36) Muller, C.; Michel, V.; Scacchi, G.; Côme, G M. J. THERGAS: A computer program for the evaluation of thermochemical data of molecules and free radicals in the gas phase. *J. Chem. Phys.* **1995**, *92*, 1154−1178.
(37) Ritter, E. R.; Bozzelli, J. THERM: Thermodynamic property estimation for gas phase radicals and molecules. *Int. J. Chem. Kinet.* **1991**, *23*, 767−778.
(38) Nguyen, T. L.; Dils, B.; Carl, S. A.; Vereecken, L.; Peeters, J. Experimental and theoretical studies of the C_2F_4 + O reaction: Nonadiabatic reaction mechanism. *J. Phys. Chem. A* **2005**, *109*, 9786−9794.
(39) Orkin, V. L.; Louis, F.; Huie, R. E.; Kurylo, M. J. Photochemistry of bromine-containing fluorinated alkenes: Reactivity toward OH and UV spectra. *J. Phys. Chem. A* **2002**, *106*, 10195−10199.
(40) Butkovskaya, N. I.; Larichev, M. N.; Leipunskii, I. O.; Morozov, I. I.; Talroze, V. L. Mass-spectrometric study of the recombination of atomic fluorine with CF_3 radicals and CF_2 biradicals. *Kinet. Catal.* **1980**, *21*, 263−267.
(41) Matheson, I.; Tedder, J. Photolysis of carbon tetrachloride in the presence of alkanes. *Int. J. Chem. Kinet.* **1982**, *14*, 1033−1045.
(42) Szirovicza, L.; Woog, J.; Bardi, I. Pyrolysis of pentanes in the presence of CCl_4, II. Kinetics of the reaction $C_2H_5 + CCl_4 \rightarrow C_2H_5Cl + CCl_3$. *Acta Chim. Acad. Sci. Hung.* **1989**, *126*, 117−122.
(43) Huybrechts, G.; Narmon, M.; Van Mele, B. The pyrolysis of CCl_4 and C_2Cl_6 in the gas phase. Mechanistic modeling by thermodynamic and kinetic parameter estimation. *Int. J. Chem. Kinet.* **1996**, *28*, 27−36.
(44) Weissman, M.; Benson, S. W. Mechanism of pyrolysis of C_2Cl_6. *Int. J. Chem. Kinet.* **1980**, *12*, 403−415.
(45) Benson, S. W.; Weissman, M. Mechanism of the pyrolysis of C_2HCl_5, molecular and radical steps. *Int. J. Chem. Kinet.* **1982**, *14*, 1287−1304.
(46) Tomkinson, D. M.; Pritchard, H. O. Abstraction of halogen atoms by methyl radicals. *J. Phys. Chem.* **1966**, *70*, 1579−1581.
(47) Goldfinger, P.; Noyes, R. M.; Wen, W. Y. The gas phase chlorine plus hydrogen bromide reaction. A bimolecular reaction of diatomic molecules. *J. Am. Chem. Soc.* **1969**, *91*, 4003−4004.
(48) Clyne, M. A. A.; Monkhouse, P. B.; Townsend, L. W. Reactions of O ^3P_j atoms with halogens: The rate constants for the elementary reactions O + BrCl, O + Br_2, and O + Cl_2. *Int. J. Chem. Kinet.* **1976**, *8*, 425−449.
(49) Evans, B. S.; Whittle, E. The kinetics of the reactions of methyl radicals with Br_2, Cl_2, and BrCl. *Int. J. Chem. Kinet.* **1978**, *10*, 745−757.
(50) Kukui, A.; Kirchner, U.; Benter, Th.; Schindler, R. N. A gas kinetic investigation of HOBr reactions with Cl(^{2}P), O(^{3}P) and OH($^2\pi$). The reaction of BrCl with OH($^2\pi$). *Ber. Bunsen-Ges. Phys. Chem.* **1996**, *100*, 455−461.
(51) Tedder, J. M.; Walton, J. C. Free radical addition to olefins. Part 12—Addition of bromodifluoromethyl radicals to fluoroethylenes. *J. Chem. Soc., Faraday Trans. 1* **1974**, *70*, 308−319.
(52) Park, J.-Y.; Slagle, I. R.; Gutman, D. Kinetics of the reaction of chlorine atoms with vinyl bromide and its use for measuring chlorine-atom concentrations. *J. Phys. Chem.* **1983**, *87*, 1812−1818.
(53) Dobis, O.; Benson, S. W. Kinetics of Cl atom reactions with C_2H_6, C_2H_5, and C_2H_4. Rates of disproportionation and recombination of ethyl radicals. *J. Am. Chem. Soc.* **1990**, *112*, 1023−1029.
(54) Baulch, D. L.; Duxbury, J.; Grant, S. J.; Montague, D. C. Evaluated kinetic data for high temperature reactions. Volume 4: Homogeneous gas phase reactions of halogen- and cyanide- containing species. *J. Phys. Chem. Ref. Data*, **1981**, *10* (Suppl. 1).
(55) Codnia, J.; Azcárate, M. L. Rate measurement of the reaction of CF_2Cl radicals with O_2. *Photochem. Photobiol.* **2006**, *82*, 755−762.

DOI: 10.1021/acs.jpca.5b00959
J. Phys. Chem. A XXXX, XXX, XXX−XXX

(56) Babushok, V.; Noto, T.; Burgess, D. R. F.; Hamins, A.; Tsang, W. Influence of CF_3I, CF_3Br, and CF_3H on the high-temperature combustion of methane. *Combust. Flame* **1996**, *107*, 351−367.
(57) Manion, J. A.; Louw, R. Thermolysis of vinyl chloride in nitrogen; rates and products between 601−681 °C. *Recl. Trav. Chim. Pays-Bas* **1986**, *105*, 442−448.
(58) Crespo, M. T.; Figuera, J. M.; Menendez, V. An estimation of the high pressure limit rate constant for the radical scission of the C−Br bond in the vinyl bromide. *An. Quim., Ser. A* **1985**, *81*, 391−394.
(59) Noto, T.; Babushok, V. I.; Hamins, A.; Tsang, W. Inhibition effectiveness of halogenated compounds. *Combust. Flame* **1998**, *112*, 147−160.
(60) Hall, J. M.; Petersen, E. L. An optimized kinetics model for OH chemiluminescence at high temperatures and atmospheric pressures. *Int. J. Chem. Kinet.* **2006**, *38*, 714−724.
(61) Westbrook, C. K. Numerical modeling of flame inhibition by CF_3Br. *Combust. Sci. Technol.* **1983**, *34*, 201−225.
(62) Casias, C. R.; McKinnon, J. T. A modeling study of the mechanisms of flame inhibition by CF_3Br fire suppression agent. *Proc. Combust. Inst.* **1998**, *27*, 2731−2739.
(63) Faeth, G. M.; Kim, C. H.; Kwon, O. C. Mechanisms of fire suppression by halons and halon replacements: A review. *Clean Air* **2003**, *4*, 115−186.
(64) Walravens, B.; Battin-Leclerc, F.; Côme, G. M.; Baronnet, F. Inhibiting effect of brominated compounds on oxidation reactions. *Combust. Flame* **1995**, *103*, 339−342.

DOI: 10.1021/acs.jpca.5b00959
J. Phys. Chem. A XXXX, XXX, XXX−XXX